

Hydration, Structure, and Molecular Interactions in the Headgroup Region of Dioleoylphosphatidylcholine Bilayers: An Electron Spin Resonance Study

Mingtao Ge and Jack H. Freed

Department of Chemistry and Chemical Biology, Baker Laboratory, Cornell University, Ithaca, New York 14853

ABSTRACT The relationship between bilayer hydration and the dynamic structure of headgroups and interbilayer water in multilamellar vesicles is investigated by electron spin resonance methods. Temperature variations of the order parameter of a headgroup spin label DPP-Tempo in DOPC in excess water and partially dehydrated (10 wt % water) show a cusp-like pattern around the main phase transition, T_c . This pattern is similar to those of temperature variations of the quadrupolar splitting of interbilayer D_2O in PC and PE bilayers previously measured by 2H NMR, indicating that the ordering of the headgroup and the interbilayer water are correlated. The cusp-like pattern of these and other physical properties around T_c are suggestive of quasiscritical fluctuations. Also, an increase (a decrease) in ordering of DPP-Tempo is correlated with water moving out of (into) interbilayer region into (from) the bulk water phase near the freezing point, T_f . Addition of cholesterol lowers T_f , which remains the point of increasing headgroup ordering. Using the small water-soluble spin probe 4-PT, it is shown that the ordering of interbilayer water increases with bilayer dehydration. It is suggested that increased ordering in the interbilayer region, implying a lowering of entropy, will itself lead to further dehydration of the interbilayer region until its lowered pressure resists further flow, i.e., an osmotic phenomenon.

INTRODUCTION

Lipid hydration and its effect on the structure of lipid bilayers is a fundamental problem in membrane biophysics (Bechinger and Seelig, 1991; Ho et al., 1995; Binder et al., 1998). In particular, lipid hydration is known to strongly affect molecular interactions in the headgroup region (Rand and Parsegian, 1989; Israelachvili and Wennerstrom, 1992). This study is directed to explore these matters by means of electron spin resonance (ESR) methods.

Anomalies in lipid bilayer hydration around the main phase transition

We have been intrigued by the anomalous hydration behavior of lipid bilayers around the main phase transition, i.e., the transition between gel and liquid crystalline phases. The first observation is that the repeat distances (lamellar lattice constants) of dipalmitoyl- and dimyristoylphosphatidylcholine (DPPC and DMPC) bilayers around the main

phase transition temperatures (T_c), measured by x-ray and neutron diffraction, were found to be 3–5 Å larger than those below and above the transition regions (Inoko and Mitsui, 1978; Rand et al., 1975; Honger et al., 1994). This is known as “anomalous swelling.” It has been interpreted by several workers as resulting from increased hydration of the headgroups, but with some differences in detail. That is, it was interpreted either as an entropy-driven swelling of bilayers as a result of reduced bilayer bending modulus (Honger et al., 1994), or as “pseudocritical behavior” involving unbinding of bilayers (Lemmich et al., 1995), or as a critical swelling of bilayers (Chen et al., 1997; Richter et al., 1999). On the other hand, it was attributed to a critical straightening of hydrocarbon chains by Zhang et al. (1995). There is, however, a consensus that the main phase transition in these PC bilayers is first order but in the vicinity of a critical point, which yields “quasiscritical” fluctuations in physical properties near T_c .

A second observation, which is the opposite of the anomalous swelling of DPPC and DMPC bilayers, is that dioleoylphosphatidylcholine (DOPC) bilayers exhibit an “anomalous shrinkage” around the main phase transition temperature, T_c , (-18°C). As is shown in Fig. 1 (Fig. 6 in Gleeson et al. (1994)), upon cooling from 20°C to $\sim -12^\circ\text{C}$, which is the freezing temperature of bulk water in equilibrium with DOPC vesicles, (T_f), the repeat distance of DOPC vesicles measured by x-ray diffraction increases only slightly from 61 Å to 64 Å. But below -12°C , the repeat distance drops precipitously from 64 Å at -12°C to 54 Å at -15°C , ($\sim 3^\circ\text{C}$ above T_c). Upon further cooling, it recovers to 60 Å at -25°C . Below -25°C it remains nearly unchanged. Upon heating, below T_c the repeat distance changes nearly reversibly, but above T_c a hysteresis in the increase of the repeat distance is observed. These changes were interpreted

Submitted March 13, 2003, and accepted for publication July 11, 2003.

Address reprint requests to Jack H. Freed, E-mail: jhf@msc.cornell.edu.

Abbreviations used: DH, dehydrated; DLPC, dilauroylphosphatidylcholine; DLPE, dilauroylphosphatidylethanolamine; DMPC, dimyristoylphosphatidylcholine; DOPC, dioleoylphosphatidylcholine; DPPC, dipalmitoylphosphatidylcholine; DPPE, dipalmitoylphosphatidylethanolamine; DPP-Tempo, 4-O-(1,2-dipalmitoyl-*sn*-glycero-3-phospho) 4-hydroxy-2,2,6,6-tetramethyl-piperidine-1-oxy; DSC, differential scanning calorimetry; DSPC, distearoylphosphatidylcholine; ESR, electron spin resonance; FH, fully hydrated; MOMD, microscopically ordered and macroscopically disordered; NLLS, nonlinear least-squares; PEG, polyethylenglycol; POPC, 1-palmitoyl-2-oleoylphosphatidylcholine; PS, phosphatidylserine; 4-PT, 4-phosphono-oxy-2,2,6,6-tetramethyl-piperidine-1-oxy; T_c , main phase transition temperature of lipid bilayers; T_f , freezing temperature; 10WT, 10 wt % of water.

© 2003 by the Biophysical Society

0006-3495/03/12/4023/18 \$2.00

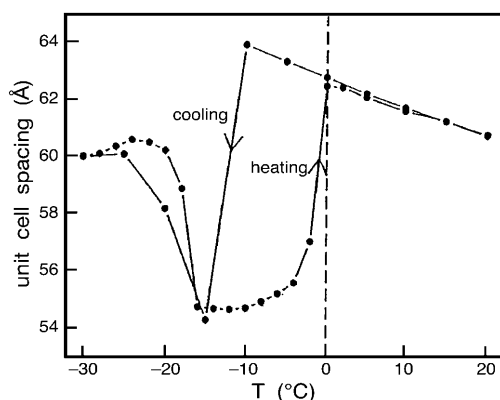


FIGURE 1 Repeat distance of DOPC vesicles in excess water as a function in temperature (from Fig. 6 in Gleeson et al. (1994)).

as resulting from water movement between the interbilayer region and the bulk water phase (ice) driven by variations in the hydration forces (Gleeson et al., 1994).

A third observation is that ^2H NMR measurements have shown an “anomalous disordering” of the interbilayer water around the main phase transition. That is, the quadrupolar splittings ($\Delta\nu$) of interbilayer D_2O molecules in PC and PE vesicles near T_c show a minimum, which is nearly zero (Pope et al., 1981; Hawton and Doane, 1987; Bryant et al., 1992). The data for DMPC, DPPC, and DMPE are shown in Fig. 2 (Fig. 1 in Hawton and Doane (1987)). This anomaly was ascribed to a fluctuation phenomenon (Hawton and Doane, 1987; Bryant et al., 1992) or to a pretransition effect (Pope et al., 1981). However, little is known how, if at all, it is related to the anomalous swelling of the bilayers.

Taken together, these anomalies strongly suggest that lipid bilayers undergo a significant structural rearrangement in the headgroup and possibly in the acyl chain regions around the main phase transition over a temperature range of $>10^\circ\text{C}$.

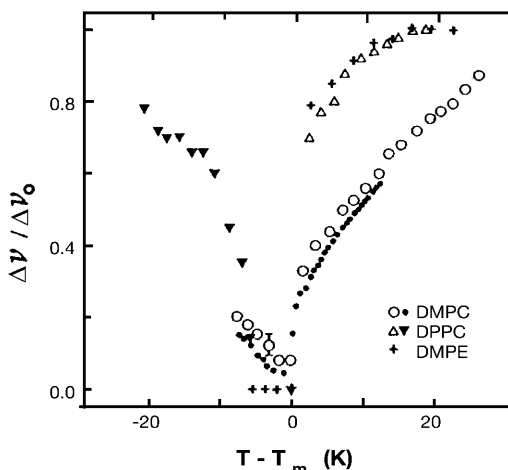


FIGURE 2 Normalized D_2O quadrupolar splitting versus $T - T_c$ for DMPC, DPPC, and DMPE. T_c was taken as 23°C for DMPC, 41°C for DPPC, and 50°C for DMPE (from Fig. 1 in Hawton and Doane (1987)).

(This includes the pretransition as well for DMPC and DPPC.) Generally, this transition has been considered to be a melting of the hydrocarbon chains (Nagle, 1980). It behaves primarily like a first order phase transition but possesses some characteristics of a second order phase transition (Papahadjopoulos et al., 1973; Wu and McConnell, 1973; Doniach, 1978; Nagle and Scott, 1978; Mitaku et al., 1983). However, the molecular detail of this transition is still not clear. In particular, much less is clear about the structure and phase behavior in the headgroup region than in the acyl chain region, undoubtedly because molecular interactions in the headgroup region are more complex than in the acyl chain region. We believe that this lack of knowledge hampers our understanding of the main phase transition of bilayers. Elucidation of these anomalies would not only shed light on the molecular mechanism of the main phase transition of lipid bilayers, but would also enhance our understanding of hydration properties of lipid bilayers, which is of fundamental importance to studies in membrane biophysics and related biological sciences.

An impetus from studies of structure in the headgroup region

Membrane fusion (including exocytosis, viral infection, and fertilization) has received long-standing interest because of its biological significance. Yet its molecular mechanism is not well understood. It has been known that polyethylene glycol (PEG) promotes membrane fusion through membrane dehydration. Arnold et al. (1987) demonstrated that this effect is mediated by increases in ordering of membrane surface water. Namely, the ordering of interbilayer deuterated water in DPPC/ D_2O dispersions increases with the concentration of PEG in the bulk water phase. These changes are correlated with a decrease in the number of interbilayer D_2O molecules bound to each DPPC molecule (Arnold et al., 1987). This finding reveals a correlation between the degree of hydration of bilayers and the structure (ordering, entropy) of interbilayer water, which is closely associated with fusogenicity of membranes. It would be very interesting to find out how the structure of headgroups affect membrane fusion. Actually this raises the following question: are the structures of membrane surface water and headgroups related to each other?

Recent molecular dynamics studies showed that in fully hydrated DMPC bilayers, the headgroups are extensively charge paired and hydrogen bonded with water molecules, forming a network structure in the headgroup region (Pasenkiewicz-Gierula et al., 1997, 1999). Even in a crystal of DMPC dihydrate, phosphate groups from two monolayers are linked together by a highly ordered water ribbon, and two adjacent phosphate groups in the same monolayer are bridged by a water molecule (Hauser et al., 1981). Thus, we would expect that the ordering of the water and the headgroups are strongly coupled. However, we were puzzled

by the result that a minimum in the quadrupolar splitting of the C-D bond in the PO-CD₂-CD₂-N group at the T_c of DPPC bilayers was not observed (Brown and Seelig, 1978), which is not consistent with the minimum ordering of interbilayer water around T_c mentioned above. Clarification of this inconsistency would enable us to better understand the structure in the headgroup region, and might also add insight to the mechanism of membrane fusion.

Aim, approach, and findings of this study

The general objectives of this study are to unravel the anomalous hydration behavior of lipid bilayers around the main phase transition, to explore how the hydration of lipid bilayers is related to the structure (ordering) of interbilayer water and headgroups.

We carried out an ESR spin labeling study on DOPC model membranes that contain either excess or 10 wt % water. Two spin labels, a headgroup labeled PC, 4-O-(1,2-dipalmitoyl-*sn*-glycero-3-phospho) 4-hydroxy-2,2,6,6-tetramethyl-piperidine-1-oxy (DPP-Tempo), and a water soluble spin label 4-phosphono-oxy-Tempo (4-PT), were incorporated into the membranes. Their chemical structures are shown in Fig. 3. The exact conformation of the phosphoryl-Tempo group in DPP-Tempo is not known. However, the phosphoryl-Tempo group in DPP-Tempo has the same chemical structure as the spin label 4-PT, which is very soluble in water, and is insoluble in the acyl chain region (Ge et al., 2001). It is likely that the phosphoryl-Tempo group

in DPP-Tempo will extend fully into the polar region. We present evidence for this from our ESR measurements discussed below. In addition, the Tempo moiety is attached to the phosphate group with a single C-O bond, around which it can rotate freely. Therefore, DPP-Tempo must be very sensitive to changes in the ordering of its surroundings in the headgroup region. ESR spectra from these spin labels in DOPC vesicles were collected at temperatures around T_c and carefully analyzed with a nonlinear least-squares (NLS) fitting program (Budil et al., 1996) based on the stochastic-Liouville equation (Schneider and Freed, 1989).

The reasons for choosing DOPC multilamellar vesicles (dispersions) for this study are as follows: 1), No pretransition was observed for DOPC dispersions in the presence of excess water using differential scanning calorimetry (DSC) (Ulrich et al., 1994). It is confirmed by our own DSC measurements (data not shown). This simplifies the study. 2), The x-ray diffraction data of DOPC dispersions (Gleeson et al., 1994) provide important structural information on the main phase transition of DOPC bilayers. By comparison with these results, the interpretation of our ESR results is facilitated. 3), The T_c of DOPC is low. Thus, the motion of DPP-Tempo at temperatures around the T_c is in the slow motional regime for ESR. As a result, the ESR spectra are very sensitive to the dynamical structural changes that occur with variation in temperature.

Our findings in the present work are the following: 1), There is a disordering of the DOPC headgroups as T_c is approached with a cusp-like appearance around T_c similar to that of the quadrupolar splitting of interbilayer D₂O in PC and PE bilayers (Hawton and Doane, 1987). This implies that the ordering of the headgroup and the ordering of the interbilayer water are correlated. 2), Changes in the ordering of the interbilayer water are associated with water movement between interbilayer and bulk water regions near T_f . Also, water moving out of (into) the interbilayer region into (from) the bulk water is accompanied by an increase (a decrease) in the ordering of headgroups. To interpret these observations we suggest an osmotic model. 3), The cusp-like pattern of ordering of the headgroups is also similar to that of the enhancement in permeability of Na⁺ (Papahadjopoulos et al., 1973) and electric conductivity (Wu and McConnell, 1973) of lipid bilayers around the main phase transition, which is suggestive of "quasicritical" fluctuations near T_c . Such fluctuations show a correlation between reduced ordering and increased hydration observed near T_c , which is consistent with the prediction of the osmotic model.

MATERIALS AND METHODS

Materials and sample preparation

DOPC was purchased from Avanti (Alabaster, AL). DPP-Tempo was custom synthesized by Nutrimed Biotech (Ithaca, NY), and 4-PT is a product of Aldrich (Milwaukee, WI).

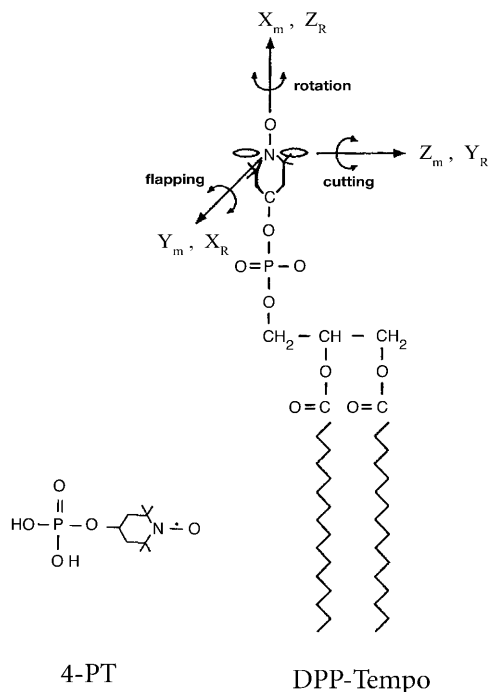


FIGURE 3 Chemical structures of DPP-Tempo (and the axis frames used in NLS simulation) and 4-PT.

Measured stock solutions of DOPC and DPP-Tempo (both in chloroform) were mixed. The concentration of DPP-Tempo was 0.5 mol % of DOPC. The solvent was evaporated by N_2 flow, then the sample was evacuated with a mechanical pump overnight to remove traces of the solvent. Two types of DOPC dispersion sample with different water content were made. For the preparation of dispersions containing 10 wt % of water, the calculated amount of deionized water was added to 50 mg dried DOPC/DPP-Tempo mixture. Then the dispersion in a sealed container was kept at 4°C for two days for equilibration. For the preparation of dispersions with excess water, 2 ml of 50 mM Tris buffer (pH 7.0, 10 mM NaCl, and 0.1 mM EDTA) were added to 2 mg dried sample, which was hydrated for at least 2 h. Both types of sample (~1.5 mg) were transferred to a capillary (0.8–1.1 mm inner diameter). For the sample with excess water, the supernatant in the capillary is 3–5 mm in length. Then the capillary was sealed for ESR measurements. Dispersions of DOPC/DPP-Tempo containing 1.0 and 10 mol % cholesterol with excess water and DOPC/4-PT with excess water were prepared in a similar manner. Differential scanning calorimetry (DSC) measurements of pure DOPC and DOPC containing 1.0 and 10 mol % cholesterol were performed on a Perkin-Elmer (Norwalk, CT) DSC-4 spectrometer.

ESR spectroscopy and nonlinear least-squares fit of ESR spectra

ESR spectra were obtained on a Bruker Instruments EMX ESR spectrometer at a frequency of 9.55 GHz equipped with a Varian temperature control unit with a temperature precision of $\pm 0.3^\circ\text{C}$.

ESR spectra from 4-PT in DOPC dispersions containing excess water were obtained from the bulk water phase and from the interbilayer region. In the former case, ESR spectra were taken from the supernatant of ~10 mm length in the capillary; (the pellet at the bottom of the capillary was far from the center of the cavity). In the latter case, the dispersion was washed with the buffer twice before it was transferred to a capillary and any supernatant was removed. DPP-Tempo is soluble only in the lipid vesicles; its ESR spectra are generated from spin labels incorporated in the DOPC bilayers. The freezing temperature of DOPC dispersions with excess water can be determined in situ by the sudden loss of microwave frequency lock in the automatic frequency control (AFC) circuit, which is caused by a large decrease in the dielectric constant of the dispersion sample when the bulk water in the sample is frozen in the cooling cycle.

Nonlinear least-squares (NLLS) analyses of the spectra from DPP-Tempo and 4-PT in DOPC dispersions were performed using the latest fitting program (Budil et al., 1996), which is based on the stochastic Liouville equation (Meirovitch et al., 1982; Schneider and Freed, 1989). The spectral analyses yield two sets of parameters, the rotational diffusion tensor components R_\perp , R_\parallel , and the ordering tensor components, S_0 , S_2 . Definitions and significance of these parameters are as follows. The piperidine ring bearing the nitroxide radical in DPP-Tempo has a twisted boat conformation similar to that of the spin label tempone (Hwang et al., 1975), which has a symmetry axis parallel to both the C-O and the N-O bonds (cf. Fig. 3). This axis is a principal diffusion axis of the tempo radical. The equivalent axis in DPP-Tempo becomes the principal axis for internal rotation of the tempo group. It will be shown below by NLLS analysis that the mean orientation of the axis, i.e., the direction of preferential orientation of the phosphoryl-Tempo group, is parallel to the normal to the bilayer.

Because one end of the phosphoryl-Tempo group is attached to the backbone of the lipid molecule, with the other end free, the rotational diffusion of the nitroxide radical in DPP-Tempo, which is incorporated in bilayers, can be described as a wobbling, i.e., a relatively free internal rotation about the C-O bond, with restricted motion about axes perpendicular to this bond. For the computation of ESR spectra from DPP-Tempo undergoing these motions, four axis frames have to be introduced (Budil et al., 1996). The first axis system (x_m , y_m , z_m) is the magnetic frame, in which the g - and A -tensors are defined. The x_m axis points along the N-O bond, the z_m axis is parallel to the axis of $2p_z$ orbital of the nitrogen atom,

and the y_m axis is perpendicular to others, forming a right-handed coordinate frame. The second axis frame, the molecular diffusion frame (x_R , y_R , z_R), is defined as follows. The z_R axis is taken as the diffusion axis for internal rotation of the nitroxide radical. It is parallel to both the N-O and the C-O bonds, which is thus parallel to the x_m axis. We refer to this as an “ x ordering” nitroxide. The y_R axis is defined as the normal to the plane of piperidine ring, which is parallel to the z_m axis. With this choice of the molecular diffusion axes frame, the wobbling motion of the nitroxide radical can be resolved into the internal rotation about the C-O bond connecting it to the phosphate (as well as rotation about the acyl chain), and rocking motions around the x_R axis, referred to as a flapping motion, and around the y_R axis, referred to as a cutting motion. The third axis frame is the bilayer orienting frame, which is referred to as the director frame by Budil et al. (1996) and designated as (x_d , y_d , z_d). The z_d axis is taken to be the local normal at each point on the surface of bilayer, whereas the x_d and y_d axes are tangential to the bilayer surface, but are otherwise arbitrarily chosen (i.e., uniaxial ordering). The fourth axis frame is the laboratory frame (x_L , y_L , z_L), with its z_L axis being defined by the static magnetic field.

The rate and range of the motions are characterized by two sets of parameters. The first set consists of R_\perp and R_\parallel . R_\perp is the rate for both rocking motions, and R_\parallel is the rate for rotation of the nitroxide radical around the internal rotation axis. The second set, S_0 and S_2 are ordering tensor parameters, which characterize the range (amplitude) of motions of the nitroxide radical. S_0 is defined as follows:

$$S_0 \equiv \langle D_{00}^2 \rangle = \left\langle \frac{1}{2} (3 \cos^2 \theta - 1) \right\rangle = \int d\Omega D_{00}^2(\Omega) P(\Omega), \quad (1)$$

where D_{00}^2 is a Wigner rotation matrix element and $P(\Omega)$ is the orientational probability distribution of the nitroxide radical. $\Omega \equiv (\theta, \phi)$, θ and ϕ are polar and azimuthal angles for the orientation of the z_R diffusion axis relative to the (x_d , y_d , z_d) local orienting potential frame. Generally, the orientational restriction of the nitroxide radical is not axially symmetric about the z_R axis. This nonaxiality is characterized by the nonaxial order parameter S_2 , which is defined in a similar manner as: $S_2 \equiv \langle D_{02}^2 + D_{0-2}^2 \rangle = \langle \sqrt{3/2} \sin^2 \theta \cos 2\phi \rangle$. The larger the value of S_0 , the smaller is the average angular amplitude of wobbling. That is, the z_R axis of the nitroxide radical is oriented more strongly along the normal to the bilayer. For a positive (negative) value of S_2 , a larger S_2 implies that the x_R (y_R) axis is more oriented along the normal to the bilayer than is the y_R (x_R) axis, which means that the amplitude of the cutting (flapping) motion is greater than that of the flapping (cutting) motion.

MOMD model

The introduction of the MOMD model, which stands for microscopically ordered but macroscopically disordered (Meirovitch et al., 1984), is based upon the characteristics of lipid vesicles. In simple terms, they are locally ordered but globally disordered. Therefore, an ESR spectrum of DPP-Tempo in DOPC vesicles is composed of component spectra from DPP-Tempo incorporated in all the domains with random orientations. The MOMD model is included in the NLLS program, so that the rotational diffusion rates and the order parameters of DPP-Tempo in DOPC dispersions can be obtained by fitting the spectrum.

Uncertainty in NLLS fitting

The uncertainties for all fitting parameters were determined by the NLLS program after the least-square minimization converged (Budil et al., 1996). Usually in a good fit with a small value of χ^2 , the uncertainty in the fitting parameters is <5%. But, this is not a sufficient criterion, because such a fit does not always reproduce all the features in the experimental spectrum. In a region where the slope of the spectrum is small, some shoulders or lumps

will often not be reproduced, because the contribution from this region of spectrum to the χ^2 is small. Therefore, the criteria for a good simulation should be small uncertainties of fitting parameters (<5%), low χ^2 and good agreement between the details of the final simulation and the experimental spectrum. All the fits in this work meet the above criteria. The main problem of simulating ESR spectra of lipid dispersions is the ambiguity that is caused by the limited resolution of MOMD type spectra generated from lipid dispersions, even though spectral simulations have met the criteria for good fit (Ge and Freed, 1999). This means that there may be more than one local minimum to which the least-squares minimization converges. To combat this ambiguity, spectra were collected as a function of temperature with small temperature steps and we required that the temperature-dependent fits be consistent. This imposes greater constraints on the simulations. For spin label DPP-Tempo in DOPC dispersions in excess water, we collected 17 spectra in a cooling cycle (from -3.7 to -25.6°C) and 21 spectra in a heating cycle (from -25.0 to -4.5°C). Our results from the simulations are generally consistent with the results from x-ray diffraction and ^2H NMR measurements, as will be shown below.

RESULTS

There are two distinct stages of variation of dynamic structure of the headgroup with temperature

ESR spectra of DPP-Tempo in DOPC dispersions with excess water were taken mainly over the range from -5.0°C to -25.0°C in both cooling and heating cycles. During the cooling cycle we observed, at temperatures between -12°C and -13°C , that the diode-detector current of the ESR spectrometer suddenly shifted, and the tuning of the cavity was lost requiring retuning. These were signs of freezing of the bulk water of the DOPC dispersion sample (recall $T_f = -12^\circ\text{C}$), which significantly changes the resonator quality factor. Plotted in Fig. 4 are the spectra at selected temperatures (*solid lines*) and simulations (*dotted lines*) obtained from NLLS fits. All spectra were fit with only a single component. As shown in Fig. 4, the agreement between the experimental and simulated spectra is very good. ESR spectra of DPP-Tempo in DOPC dispersions with 10 wt % water were collected from 1.1°C down to -13.2°C in the cooling cycle and from -14.5°C up to 1.6°C in the heating cycle (spectra not shown). The best fit values of rotational diffusion rates, R_\perp , R_\parallel , and order parameters, S_0 , S_2 for dispersions containing excess water are listed in Tables 1 and 2 for cooling and heating cycles, respectively. Corresponding values for dispersions containing 10 wt % water are listed in Tables 3 and 4 for cooling and heating cycles, respectively. We note that ^2H NMR spectra from deuterated PC, ^{13}C NMR spectra from ^{13}C labeled PC, and ESR spectra from spin labeled stearic acid in the ripple phase of pure PC bilayers all consist of two components (Westerman et al., 1982; Wittebort et al., 1982; Tsuchida and Hatta, 1988). Although our DSC experiment did not show a pretransition in DOPC bilayers, we did observe two-component ESR spectra from the spin label 5PC in DOPC dispersion with excess water around the main phase transition (unpublished data). It is quite possible that the ESR spectra from DPP-

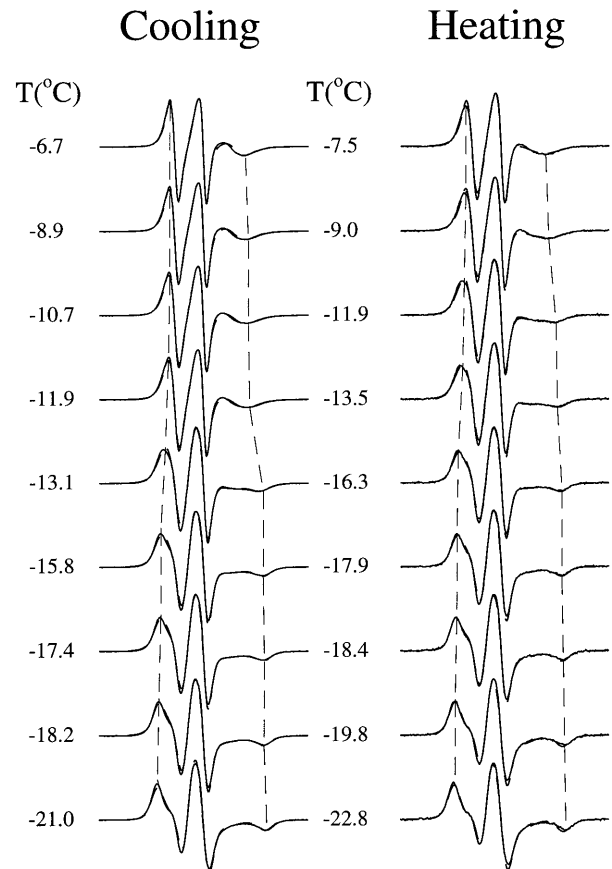


FIGURE 4 Selected ESR spectra of DPP-Tempo in DOPC dispersion with excess water in cooling and heating cycles. Solid lines: experimental; dashed lines: simulations.

Tempo in DOPC dispersions shown in Fig. 4 are composed of two components, which are not resolved. Thus, the best fit parameters listed in Tables 1–4 might be weighted averages of parameters of two components.

In the Introduction we mentioned that the phosphoryl-Tempo group should be aligned with its z_R axis parallel to the normal to the bilayer, i.e., z_d axis. This can be readily inferred from the NLLS fits as follows. Our results have shown that the fastest rotation of the nitroxide radical (R_\parallel) is about the x_m axis, as expected from internal rotation about the C-O bond. We also find that this is the axis that is well aligned with respect to the local director of the bilayer z_d , because of the positive order parameters S_0 , whereas the y_m and z_m axes are ordered perpendicular to it. Because the dominant ordering in a membrane is along the membrane normal (i.e., parallel to the acyl chains), it seems reasonable to take this local director along the membrane normal. (If x_m were aligned in a direction perpendicular to z_d , it would have yielded a large negative ordering.) For these reasons we have chosen the x_m axis as z_R and the normal to the bilayer as the director for the alignment of the Tempo group in the NLLS fits. A more accurate assessment of this matter requires

TABLE 1 Rotational diffusion rates and order parameters of spin label DPP-Tempo in DOPC dispersions in the presence of excess water (cooling cycle)

T (°C)	R_{\perp} (s ⁻¹)	R_{\parallel} (s ⁻¹)	S_0	S_2
-25.6	1.00×10^5	2.69×10^7	0.752	-0.116
-23.7	1.00×10^5	3.55×10^7	0.686	-0.170
-21.0	1.00×10^5	5.62×10^7	0.535	-0.281
-19.6	8.71×10^5	7.41×10^7	0.458	-0.343
-18.2	1.48×10^6	7.08×10^7	0.555	-0.279
-17.4	2.24×10^6	7.94×10^7	0.552	-0.281
-16.6	2.04×10^6	8.13×10^7	0.561	-0.274
-15.8	2.45×10^6	8.32×10^7	0.578	-0.261
-15.0	2.75×10^6	8.71×10^7	0.579	-0.263
-13.1	3.98×10^6	1.02×10^8	0.573	-0.262
-11.9	7.08×10^6	1.17×10^8	0.295	-0.174
-10.7	7.76×10^6	1.23×10^8	0.294	-0.172
-9.6	8.51×10^6	1.32×10^8	0.296	-0.175
-8.9	9.12×10^6	1.35×10^8	0.307	-0.174
-7.7	9.33×10^6	1.51×10^8	0.307	-0.179
-6.7	1.05×10^7	1.58×10^8	0.307	-0.179
-3.7	1.20×10^7	2.04×10^8	0.295	-0.191

The magnetic parameters used in the simulations: $g_{xx}, g_{yy}, g_{zz} = 2.0090, 2.0062, 2.0020$, and $A_{xx}, A_{yy}, A_{zz} (G) = 6.1, 6.1, 34.3$. The least squares estimated errors in R_{\perp} and $R_{\parallel} < \pm 5\%$; in S_0 and $S_2, \pm 0.003$.

a consideration of the phase biaxiality of the local ordering potential (Barnes and Freed, 1998) resulting from acyl chain alignment as well as local headgroup alignment.

The preferred orientation of the nitroxide moiety can be shown more conveniently by the Cartesian order parameters (see Appendix A) than by the order parameters S_0 and S_2 , which are irreducible spherical tensors components. For example, at -13.1°C (cooling cycle) the order parameters of

TABLE 2 Rotational diffusion rates and order parameters of spin label DPP-Tempo in DOPC dispersions in the presence of excess water (heating cycle)

T (°C)	R_{\perp} (s ⁻¹)	R_{\parallel} (s ⁻¹)	S_0	S_2
-25.0	1.00×10^5	2.24×10^7	0.761	-0.116
-22.0	1.00×10^5	3.47×10^7	0.642	-0.199
-19.0	1.35×10^6	5.25×10^7	0.424	-0.350
-18.4	1.62×10^6	7.08×10^7	0.467	-0.333
-17.9	2.29×10^6	7.08×10^7	0.529	-0.287
-17.3	2.29×10^6	7.59×10^7	0.552	-0.272
-16.7	2.63×10^6	7.59×10^7	0.569	-0.257
-16.3	2.57×10^6	8.13×10^7	0.560	-0.268
-15.0	3.47×10^6	8.91×10^7	0.566	-0.260
-14.5	3.72×10^6	8.91×10^7	0.565	-0.261
-13.5	4.17×10^6	1.00×10^8	0.559	-0.263
-13.0	4.57×10^6	1.02×10^8	0.555	-0.266
-11.9	5.13×10^6	1.10×10^8	0.557	-0.248
-11.0	5.25×10^6	1.17×10^8	0.516	-0.238
-9.5	5.25×10^6	1.26×10^8	0.406	-0.234
-8.5	5.50×10^6	1.45×10^8	0.340	-0.245
-8.0	5.62×10^6	1.51×10^8	0.310	-0.244
-7.5	5.89×10^6	1.62×10^8	0.291	-0.248
-6.0	6.46×10^6	1.91×10^8	0.233	-0.248
-4.5	7.41×10^6	2.29×10^8	0.207	-0.250

The magnetic parameters used in the simulations: $g_{xx}, g_{yy}, g_{zz} = 2.0090, 2.0062, 2.0020$, and $A_{xx}, A_{yy}, A_{zz} (G) = 6.1, 6.1, 34.3$. The least squares estimated errors in R_{\perp} and $R_{\parallel} < \pm 5\%$; in S_0 and $S_2, \pm 0.003$.

TABLE 3 Rotational diffusion rates and order parameters of spin label DPP-Tempo in DOPC dispersions containing 10 wt % water (cooling cycle)

T (°C)	R_{\perp} (s ⁻¹)	R_{\parallel} (s ⁻¹)	S_0	S_2
-13.2	1.00×10^5	5.25×10^7	0.679	-0.202
-10.3	1.15×10^5	6.76×10^7	0.642	-0.234
-8.6	1.00×10^5	7.59×10^7	0.624	-0.247
-7.7	1.66×10^6	7.59×10^7	0.555	-0.278
-6.3	2.09×10^6	7.76×10^7	0.573	-0.267
-4.8	2.40×10^6	8.32×10^7	0.577	-0.262
-3.7	2.82×10^6	8.71×10^7	0.582	-0.258
1.1	5.01×10^6	9.77×10^7	0.611	-0.231

The magnetic parameters used in the simulations: $g_{xx}, g_{yy}, g_{zz} = 2.0090, 2.0062, 2.0020$, and $A_{xx}, A_{yy}, A_{zz} (G) = 6.15, 6.15, 34.3$. The least squares estimated errors in R_{\perp} and $R_{\parallel} < \pm 5\%$; in S_0 and $S_2, \pm 0.003$.

DPP-Tempo in the DOPC dispersion containing excess water S_0 and S_2 are 0.573 and -0.262 respectively. The corresponding Cartesian order parameters are: $S_{zz} = S_0 = 0.573$, $S_{xx} = (1/2)\sqrt{3/2}S_2 - (1/2)S_0 = -0.447$, $S_{yy} = -(1/2)\sqrt{3/2}S_2 - (1/2)S_0 = -0.126$. The large positive S_{zz} indicates that the principal diffusion axis of Tempo (z_R) is strongly oriented along the local director, normal to the bilayers, as we have just discussed. The large negative S_{xx} , almost -0.5 , indicates that the x_R axis of Tempo is confined to be perpendicular to the director, whereas a less negative S_{yy} indicates that the y_R axis is less strongly confined to be perpendicular to the normal to the bilayers than the x_R axis.

In Fig. 5, the parameters $R_{\perp}, R_{\parallel}, S_0$, and S_2 of DPP-Tempo in DOPC dispersions with excess water are plotted versus the temperature for both the cooling and heating cycles. There is a sharp increase in S_0 at the freezing point, $T_f, -12^{\circ}\text{C}$, i.e., from 0.295 at -11.9°C to 0.573 at -13.1°C . Below T_f , the curves of S_0 vs. T and S_2 vs. T are very similar in the cooling and heating cycles. They all exhibit cusp-like patterns, and are well superimposed with each other when plotted together, as shown in Fig. 6.

TABLE 4 Rotational diffusion rates and order parameters of spin label DPP-Tempo in DOPC dispersions containing 10 wt % water (heating cycle)

T (°C)	R_{\perp} (s ⁻¹)	R_{\parallel} (s ⁻¹)	S_0	S_2
-14.5	1.00×10^5	4.90×10^7	0.681	-0.200
-13.0	1.00×10^5	5.25×10^7	0.662	-0.215
-11.9	1.00×10^5	5.75×10^7	0.655	-0.221
-10.5	1.00×10^5	6.61×10^7	0.641	-0.235
-8.9	1.00×10^5	7.41×10^7	0.615	-0.254
-7.5	1.86×10^6	7.76×10^7	0.529	-0.291
-6.2	2.04×10^6	7.76×10^7	0.571	-0.267
-4.1	2.75×10^6	8.51×10^7	0.581	-0.258
-2.9	3.16×10^6	8.91×10^7	0.587	-0.255
-0.1	4.47×10^6	9.55×10^7	0.601	-0.236
1.6	5.13×10^6	1.02×10^8	0.600	-0.228

The magnetic parameters used in the simulations: $g_{xx}, g_{yy}, g_{zz} = 2.0090, 2.0062, 2.0020$, and $A_{xx}, A_{yy}, A_{zz} (G) = 6.15, 6.15, 34.3$. The least squares estimated errors in R_{\perp} and $R_{\parallel} < \pm 5\%$; in S_0 and $S_2, \pm 0.003$.

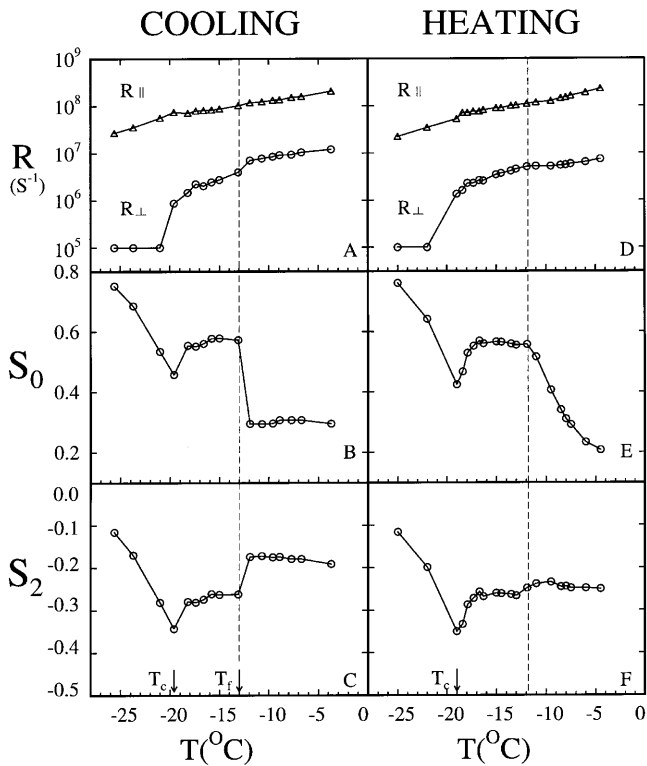


FIGURE 5 Plot of rotational diffusion rates, R_{\perp} , R_{\parallel} (A, D), order parameter S_0 (B, E), and nonaxial order parameter S_2 (C, F), of DPP-Tempo in DOPC dispersion with excess water versus temperature in cooling and heating cycles. T_c is the main phase transition temperature, and T_f is the freezing temperature. The dashed line demarcates between the transition (T) stage and the nontransition (N) stage in the change of DOPC vesicles with temperature.

The different patterns in those curves above and below -12°C indicate that there are two distinct stages in the dynamic structure of DOPC bilayers. For ease of visualization these stages are separated by a vertical dashed line in Fig. 5. For convenience, the stages on the left and on the right sides of the line are referred to as the transition stage (T stage), and the nontransition stage (N stage), respectively.

ESR spectra from DPP-Tempo in DOPC dispersions containing 10 wt % water (no bulk water present) exhibit significant changes only around T_c . In Fig. 7 the parameters R_{\perp} , R_{\parallel} , S_0 , and S_2 obtained from NLLS analysis of these spectra are plotted versus relative temperature, i.e., the difference between the experimental temperature and T_c (-7°C) for both the cooling and heating cycles.

Effect of incorporation of cholesterol

To perturb both the main phase transition and the freezing of DOPC bilayers, 1.0 and 10 mol % of cholesterol were added to the DOPC vesicles. Richter et al. (1999) have previously observed pseudocritical behavior in DMPC containing <15% sterols. In Fig. 8, A–F, the rotational diffusion rates

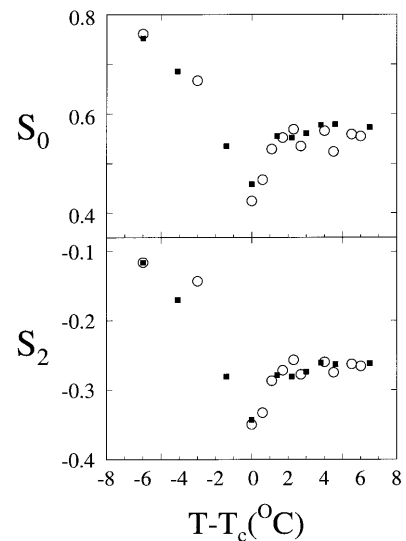


FIGURE 6 Superposition of plot of order parameters S_0 , S_2 of DPP-Tempo in DOPC dispersion with excess water around the main phase transition in heating (\blacksquare) and cooling cycles (\circ).

R_{\perp} , R_{\parallel} and the order parameters S_0 , S_2 of DPP-Tempo in DOPC dispersions containing 1.0 and 10 mol % of cholesterol obtained from NLLS fits are plotted versus T in a temperature range (cooling cycle) similar to that studied for pure DOPC. These parameters are also listed in Tables 5 and

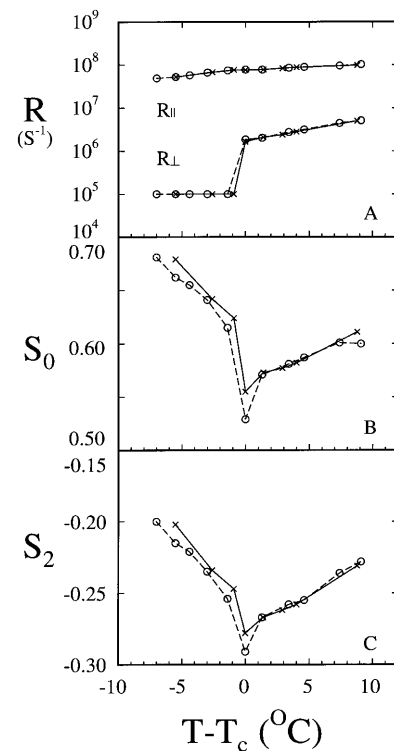


FIGURE 7 Plot of R_{\perp} , R_{\parallel} , S_0 , and S_2 of DPP-Tempo in DOPC dispersion containing 10 wt % water in heating (dashed lines) and cooling (solid lines) cycles versus the relative temperature, $T - T_c$.

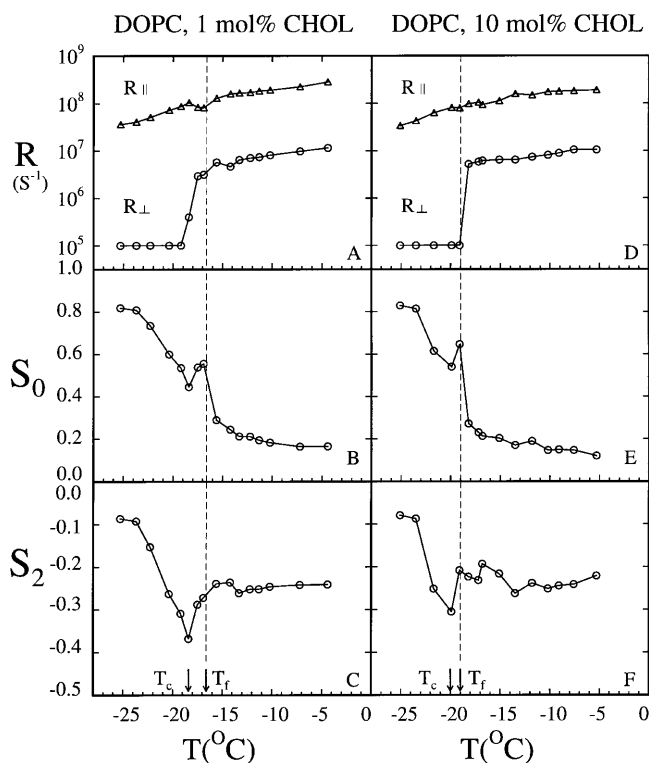


FIGURE 8 Plot of rotational diffusion rates, R_{\perp} , R_{\parallel} , order parameters S_0 , and nonaxial order parameter S_2 of DPP-Tempo in DOPC dispersion containing 1.0 (A–C) and 10 (D–F) mol % cholesterol in the presence of excess water as a function of temperature in the cooling cycle. T_c is the main phase transition temperature, and T_f is the freezing temperature. The dashed line demarcates between the transition (T) stage and the nontransition (N) stage in the change of DOPC/cholesterol vesicles with temperature.

6 for DOPC containing 1.0 and 10 mol % cholesterol, respectively. It is seen from Fig. 8 and Tables 5 and 6 that the main phase transition temperature, which is $\sim -18.4^{\circ}\text{C}$ for DOPC containing 1.0 mol % cholesterol, and $\sim -19.9^{\circ}\text{C}$ for DOPC containing 10 mol % cholesterol (confirmed by DSC, data not shown) is nearly the same as that of the pure DOPC (-19.6°C in the cooling cycle and -19.0°C in the heating cycle). Also, in both cases (DOPC containing 1.0 and 10 mol % cholesterol) S_0 and S_2 show the cusp-like pattern around T_c . Because the freezing point is lowered from -12°C to -15.6°C and -18.2°C for DOPC incorporated with 1.0 and 10 mol % of cholesterol, respectively (confirmed by DSC, data not shown), only part of the cusp-like pattern is observed. But still we can distinguish the two stages (N and T stages) for the variation of the dynamic structure. In the T stages, S_0 and S_2 are also strongly correlated as in the case of pure DOPC.

Usually, in the presence of cholesterol the main phase transition for PC bilayers is broadened (Lewis and McElhaney, 1991). However, the transition in DOPC containing 10 mol % of cholesterol remains as sharp as in pure DOPC. The above results indicate that incorporation of cholesterol into DOPC bilayers does not have a large effect

TABLE 5 Rotational diffusion rates and order parameters of spin label DPP-Tempo in DOPC dispersions containing 1.0 mol % cholesterol in the presence of excess water (cooling cycle)

T ($^{\circ}\text{C}$)	R_{\perp} (s^{-1})	R_{\parallel} (s^{-1})	S_0	S_2
-25.3	1.00×10^5	3.63×10^7	0.818	-0.087
-23.7	1.00×10^5	4.07×10^7	0.808	-0.093
-22.3	1.00×10^5	5.13×10^7	0.734	-0.153
-20.4	1.00×10^5	7.24×10^7	0.599	-0.263
-19.2	1.00×10^5	8.71×10^7	0.535	-0.309
-18.4	3.98×10^5	1.05×10^8	0.445	-0.368
-17.5	2.95×10^6	8.32×10^7	0.538	-0.288
-16.9	3.16×10^6	8.13×10^7	0.555	-0.272
-15.6	5.75×10^6	1.29×10^8	0.289	-0.239
-14.2	4.68×10^6	1.58×10^8	0.244	-0.236
-13.3	6.46×10^6	1.66×10^8	0.212	-0.261
-12.2	7.08×10^6	1.70×10^8	0.211	-0.252
-11.3	7.41×10^6	1.82×10^8	0.194	-0.252
-10.2	8.13×10^6	1.91×10^8	0.183	-0.246
-7.2	9.77×10^6	2.24×10^8	0.164	-0.242
-4.4	1.15×10^7	2.82×10^8	0.165	-0.241

The magnetic parameters used in the simulations: g_{xx} , g_{yy} , $g_{zz} = 2.0092$, 2.0064, 2.0020, and A_{xx} , A_{yy} , A_{zz} (G) = 6.1, 6.1, 34.7. The least squares estimated errors in R_{\perp} , R_{\parallel} , S_0 , and S_2 are the same as in Table 1.

on the main phase transition of DOPC bilayers. Richter et al. (1999) did find that addition of sterol to DMPC reduces the criticality of the system. It is known that cholesterol interacts strongly with PCs with at least one saturated acyl chain due to the van der Waals interaction between the planar moiety of the cholesterol molecule and the saturated acyl chains of PCs. Because both acyl chains in DOPC are unsaturated, there are no strong interactions between cholesterol and the acyl chains of DOPC. Thus, the main phase transition of DOPC bilayers is not strongly perturbed by the incorporation of cholesterol. However, we note that S_0 of

TABLE 6 Rotational diffusion rates and order parameters of spin label DPP-Tempo in DOPC dispersions containing 10 mol % cholesterol in the presence of excess water (cooling cycle)

T ($^{\circ}\text{C}$)	R_{\perp} (s^{-1})	R_{\parallel} (s^{-1})	S_0	S_2
-25.1	1.00×10^5	3.39×10^7	0.829	-0.079
-23.5	1.00×10^5	4.27×10^7	0.814	-0.087
-21.7	1.00×10^5	6.31×10^7	0.614	-0.251
-19.9	1.00×10^5	8.13×10^7	0.540	-0.305
-19.1	1.00×10^5	7.94×10^7	0.646	-0.208
-18.2	5.25×10^6	9.77×10^7	0.272	-0.223
-17.2	5.89×10^6	1.05×10^8	0.230	-0.231
-16.8	6.17×10^6	9.33×10^7	0.213	-0.193
-15.1	6.46×10^6	1.12×10^8	0.203	-0.216
-13.5	6.46×10^6	1.58×10^8	0.170	-0.262
-11.8	7.41×10^6	1.48×10^8	0.189	-0.238
-10.2	8.13×10^6	1.74×10^8	0.146	-0.251
-9.1	8.91×10^6	1.79×10^8	0.149	-0.244
-7.6	1.05×10^7	1.82×10^8	0.146	-0.241
-5.3	8.13×10^6	1.91×10^8	0.183	-0.246

The magnetic parameters used in the simulations: g_{xx} , g_{yy} , $g_{zz} = 2.0092$, 2.0064, 2.0020, and A_{xx} , A_{yy} , A_{zz} (G) = 6.1, 6.1, 34.7. The least squares estimated errors in R_{\perp} , R_{\parallel} , S_0 , and S_2 are the same as in Table 1.

DPP-Tempo decreases from 0.295 (0.207) at -3.7°C (-4.5°C) in the cooling (heating) cycle for pure DOPC to 0.165 at -4.4°C for DOPC with 1.0 mol % cholesterol, and further decreases to 0.118 for DOPC with 10 mol % cholesterol. This is consistent with the results from a 2D-ELDOR study on DPPC membranes that cholesterol decreases the ordering of lipid headgroups (Costa-Filho et al., 2003). Furthermore, as we have seen, T_f is lowered by addition of cholesterol, and the sharp increase in ordering continues to occur at T_f .

Interbilayer water is more ordered than bulk water

ESR spectra (*solid lines*) from spin label 4-PT in the bulk water phase and interbilayer region at temperatures near T_f in the cooling cycle and simulations (*dotted lines*) are shown in Fig. 9. The ESR spectra of 4-PT in the bulk water phase at all temperatures and those in interbilayer region above T_f (-12°C) can be well fitted with a single component, and those in the interbilayer region below T_f are fitted with two components. The best fit values of rotational diffusion rate, R_{\perp} and order parameters, S_0 , S_2 for 4-PT spectra in the bulk water phase and the interbilayer region are listed in Tables 7

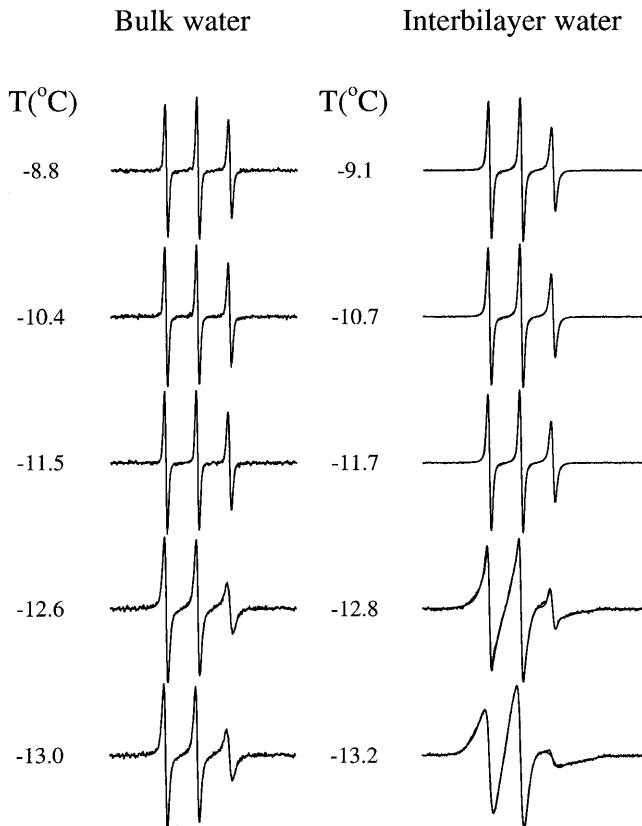


FIGURE 9 Selected ESR spectra of 4-PT in the bulk water phase and in the interbilayer region of DOPC dispersions around the freezing point.

TABLE 7 Rotational diffusion rates and order parameters of spin label 4-PT in bulk water phase in the presence of DOPC dispersions

T ($^{\circ}\text{C}$)	R_{\perp} (s^{-1})	S_0	S_2
-8.8	8.81×10^8	0.13	-0.12
-10.4	8.71×10^8	0.14	-0.12
-11.5	7.94×10^8	0.14	-0.11
-12.6	1.62×10^8	0.24	-0.17
-13.0	1.55×10^8	0.25	-0.17

The magnetic parameters used in the simulations: g_{xx} , g_{yy} , $g_{zz} = 2.0086$, 2.0064, 2.0020, and A_{xx} , A_{yy} , A_{zz} (G) = 6.80, 6.80, 37.9. The least squares estimated errors in $R_{\perp} < \pm 5\%$; in S_0 and S_2 , ± 0.01 .

and 8, respectively. (Because the simulation is not sensitive to R_{\parallel} of 4-PT, so the values of R_{\parallel} were fixed at a ratio R_{\parallel}/R_{\perp} of 2 in the simulations.) These results show considerable differences. Plotted in Fig. 10 are order parameters S_0 of 4-PT in bulk water and interbilayer regions versus the temperature. In the temperature range studied, the order parameters of 4-PT in the interbilayer region are higher than those in bulk water phase, which is nonzero (Small nitroxide probes are known to exhibit microscopic ordering in complex liquids due to local solvent structure (Earle et al., 1997)). In addition, upon cooling to T_f , the former jumps from 0.18 at -11.7°C to 0.53 (the S_0 value of the major component of 4-PT spectrum) at -12.8°C , whereas a much smaller jump of the latter (from 0.14 at -11.5°C to 0.24 at -12.6°C) was observed.

It is likely that in the interbilayer region 4-PT molecules are mainly ordered by surrounding water molecules, in which case their order parameters can be viewed as a measure of the ordering of interbilayer water. Thus, below T_f the increase in ordering of interbilayer water is much larger than that of bulk water. Such an increase in ordering of interbilayer water at T_f is thus correlated with the increased ordering of the headgroups (cf. Fig. 5).

Upon freezing, 4-PT molecules in the bulk water phase are excluded from ice crystals into the concentrated buffer solution. This is revealed by a sudden change in 4-PT spec-

TABLE 8 Rotational diffusion rates and order parameters of spin label 4-PT in the interbilayer region of DOPC dispersions in the presence of excess water

T ($^{\circ}\text{C}$)	C^{\ddagger}	R_{\perp} (s^{-1})	S_0	S_2	P^{\ddagger}
-9.9	-	4.68×10^8	0.18	-0.16	-
-10.7	-	4.47×10^8	0.17	-0.16	-
-11.7	-	4.68×10^8	0.18	-0.16	-
-12.8	1	2.34×10^7	0.53	-0.31	0.90
-	2	3.16×10^8	-0.01	-0.10	0.10
-13.2	1	5.01×10^7	0.64	-0.23	0.63
-	2	3.09×10^7	0.21	-0.43	0.37

The g -tensor and A -tensor components for 4-PT are the same as in Table 7. The least squares estimated errors in $R_{\perp} < \pm 5\%$; in S_0 and S_2 , ± 0.01 . C = component; P = population.

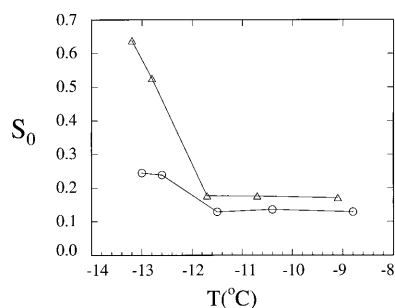


FIGURE 10 Plot of order parameters S_0 of 4-PT in the bulk water phase (○) and in the interbilayer region (△) of DOPC dispersions versus temperature.

tra from a fast motional spectrum ($R_{\perp} = 7.94 \times 10^8 \text{ s}^{-1}$ at -11.5°C) to a slower motional spectrum ($R_{\perp} = 1.62 \times 10^8 \text{ s}^{-1}$ at -12.6°C), but not to a rigid limit spectrum. Thus, the increase in the ordering of 4-PT indicates an increase in the ordering of water in the concentrated buffer solution below T_f as compared to the ordering of the bulk water above T_f . On the other hand, below T_f 4-PT molecules in the interbilayer region have a dominant component that is not only highly ordered, but exhibits much slower motion ($R_{\perp} = 2.34 \times 10^7 \text{ s}^{-1}$ at -12.8°C). ESR spectra of 4-PT in the interbilayer region at temperatures below -13°C proved very difficult to fit, so no fitting parameters are listed for them. We suspect that below -13°C the 4-PT molecules reside in a range of different microenvironments in the dehydrated interbilayer region.

An inverse correlation between headgroup ordering and degree of lipid hydration

Let us first examine changes in the ordering of DPP-Tempo in the N stage and compare them with changes in the repeat distance of DOPC bilayers in the same temperature range from the x-ray diffraction study. In the cooling cycle, as shown in Fig. 5, as the temperature decreases from -3.7°C to -11.9°C S_0 remains nearly unchanged, but increases sharply from 0.295 at -11.9°C (T_f) to 0.573 at -13.1°C (also cf. Table 1). However, the repeat distance of DOPC bilayers decreases sharply going from $\sim 64 \text{ \AA}$ at -12°C to $\sim 54 \text{ \AA}$ at -15°C by 10 \AA (cf. Fig. 1 from Gleeson et al., 1994). In the heating cycle, also as shown in Fig. 5, above -12°C S_0 decreases sharply, whereas starting from -10°C with a slight hysteresis the repeat distance of DOPC bilayers increases with temperature sharply (cf. Fig. 1 from Gleeson et al., 1994). The above comparisons reveal that in the N stage (cooling and heating cycles) the order parameters of DPP-Tempo and the repeat distance of DOPC bilayers are inversely correlated.

Because changes in the thickness of acyl chain region and in the thickness of headgroup region could both contribute to

the variation of the repeat distance, these two contributions should be discriminated. It was shown that the increase in thickness of the headgroup region in heating from -15°C to 0°C due to melting of the ice and water flowing from the bulk water region into the interbilayer region is 6.5 \AA as opposed to a total increase of 8 \AA in the repeat distance from 54.5 \AA at -15°C to 62.5 \AA at 0°C (cf. Fig. 1 and Gleeson et al., 1994), indicating that the increase in thickness of the headgroup region dominates the increase in the repeat distance. We now consider the cooling cycle. As shown in Fig. 1, the variation of repeat distance of DOPC vesicles with temperature between -15°C and -30°C is approximately reversible, whereas between -15°C and 0°C it is different in the cooling cycle versus the heating cycle, i.e., a large hysteresis effect. However, at 0°C and also at -15°C , the repeat distances are nearly the same for heating and cooling cycles, suggesting that at each of these two temperatures, the dynamic structure of the DOPC bilayers is very similar for both cycles. Thus it follows that in the cooling cycle, dehydration of the headgroups makes the major contribution to the sharp drop of the repeat distance. However, from -12°C to -15°C in the cooling cycle, only 6.5 \AA of the 10 \AA decrease in the repeat distance of DOPC bilayers is due to the dehydration of the headgroups (Gleeson et al., 1994). It implies that thinning of acyl chains also makes a smaller but significant contribution (of 3.5 \AA) to the overall decrease in repeat distance.

To summarize, dehydration of headgroups (below T_f in the cooling cycle) is correlated with the large increase in the ordering of headgroups, whereas rehydration of headgroups (above -12°C in the heating cycle) is correlated with the large decrease in the ordering of headgroups. Thus, there is an inverse correlation of headgroup ordering and hydration of the lipid bilayers.

A continuous conformational change in DOPC headgroups around the main phase transition

In the cooling cycle the T stage begins when the bulk water is frozen. Below T_f both S_0 and S_2 decrease slowly with decreasing temperature. When the temperature approaches close to the main phase transition temperature, T_c , they decrease suddenly, reaching their minima at T_c , and bound up sharply below T_c (Fig. 5, B and C). These changes in S_0 and S_2 reveal important features in the structural rearrangement in the headgroup region of DOPC bilayers during the main phase transition. They can be described as follows: 1), The two curves of S_0 and S_2 vs. T are nearly parallel, and both show a minimum at T_c (cf. Fig. 5, B and C). Thus, below T_f as the temperature decreases toward T_c , S_0 decreases and S_2 becomes more negative such that the Cartesian order parameters change from $S_{xx} = -0.447$, $S_{yy} = -0.126$, and $S_{zz} = 0.573$ at -13.1°C to $S_{xx} = -0.439$, $S_{yy} = -0.019$, and $S_{zz} = 0.458$ at -19.6°C . These results indicate that as the symmetry axis (z_R axis) of the nitroxide radical becomes less strongly oriented along the normal to

the bilayer, the y_R axis becomes less oriented tangential to the bilayer, but the x_R axis retains its strong orientation. This is a continuous change in preference of orientation of the nitroxide moiety, which is caused by a change in the orienting potential (molecular force field) in the headgroup region. It implies that the DOPC headgroup is undergoing a continuous conformational change, which will be discussed in more detail in Discussion. 2), Below T_c as the temperature further decreases, S_0 increases sharply. The headgroups are much more ordered below T_c than above T_c , and the nonaxiality of the ordering is significantly reduced (e.g., at -25.6°C , $S_{xx} = -0.447$, $S_{yy} = -0.305$, and $S_{zz} = 0.752$). The order parameters of S_0 and S_2 of DPP-Tempo in DOPC vesicles containing 10 wt % water show similar features as described above in the main phase transition range (cf. Fig. 7).

A correlation between the ordering of headgroup and the ordering of interbilayer water

The cusp-like patterns of temperature variation of S_0 and S_2 of DPP-Tempo around the main phase transition in DOPC dispersions containing excess water (Figs. 5 and 6) and 10 wt % water (Fig. 7) are very similar to those of the temperature variation of the quadrupolar splitting of interbilayer D_2O in PCs and PEs (Pope et al., 1981; Hawton and Doane, 1987; Bryant et al., 1992), as shown in Fig. 2. This leads us to suggest that the ordering of the headgroups and the ordering of the interbilayer water are correlated. This suggestion is consistent with the results that both ordering of the headgroups and of the interbilayer water are inversely correlated with the degree of hydration of lipid bilayers. In addition, the cusp-like pattern of ordering around T_c in Fig. 6 is strikingly similar to that of the behavior of the permeability of Na^+ (Papahadjopoulos et al., 1973) and the electrical conductivity (Wu and McConnell, 1973) through DPPC bilayers, which have been related to density fluctuations in the headgroup region (Nagle and Scott, 1978).

In the gel phase, motions of DOPC headgroups are not completely frozen

In the cooling cycle, upon freezing of the bulk water (entering the T stage), R_\perp decreases from $7.08 \times 10^6 \text{s}^{-1}$ at -11.9°C to $3.98 \times 10^6 \text{s}^{-1}$ at -13.1°C , i.e., by a factor of ~ 2 . In the T stage, R_\perp decreases from $8.71 \times 10^5 \text{s}^{-1}$ at -19.6°C (T_c) to $1.00 \times 10^5 \text{s}^{-1}$ at -21.0°C , i.e., by a factor of ~ 9 , and remains at $\sim 1.00 \times 10^5 \text{s}^{-1}$ below T_c (cf. Fig. 5 A and Table 1), indicating that in the gel phase of DOPC bilayers rocking motions of the nitroxide radical are virtually frozen on the ESR timescale. In contrast, R_\parallel changes with temperature very gradually in the whole temperature range studied, except near T_c , where a small break is observed. Below T_c , R_\parallel is still $> 10^7 \text{s}^{-1}$, i.e., in the gel phase internal

motions of the nitroxide moiety in the DOPC headgroup region remain significant.

For convenience, we introduce the following abbreviations for three different structures of DOPC dispersions, which will be involved in the Discussion. Dispersions that are originally prepared containing excess water will be referred to as FH (fully hydrated) DOPC dispersion, and ones that are dehydrated in the cooling cycle at temperatures below -12°C (see below) will be referred to as DH (dehydrated) DOPC dispersion. Those containing 10 wt % water will be referred to as 10WT DOPC dispersion.

DISCUSSION

Significance of the correlation between the ordering of headgroup and the ordering of interbilayer water

To adequately appreciate the significance of the correlation between the variation of order parameter of DPP-Tempo and the variation of quadrupolar splitting of interbilayer water, $\Delta\nu$, a matter previously discussed by Gawrisch et al. (1992) first needs to be reconsidered. Briefly, they noticed an apparent contradiction between a very small quadrupolar splitting of deuterated water at lipid bilayer surfaces and the much higher ordering of water molecules, as determined by membrane surface dipole potential measurements. They ascribed the small $\Delta\nu$ of D_2O to the fast rotation of the O-D bond of the water molecule around an axis that makes nearly a magic angle with the O-D bond. Similarly, we note that $\Delta\nu$ of interbilayer D_2O in PC and PE membranes containing 10 wt % or less water was reported to be $< 2 \text{ kHz}$ (Bryant et al., 1992; Pope et al., 1981), which is much smaller than the static quadrupolar splitting constant of 170 kHz, indicative of a very low ordering of the O-D bond of water. This is inconsistent with the high ordering of headgroups in bilayers of low hydration, e.g., in 10WT and DH DOPC dispersions that we have observed in our present ESR studies. In the following, we interpret the contradiction in terms of the hydrogen bonding network in the headgroup region of bilayers.

Recent molecular dynamics studies have shown that in the headgroup region, water molecules are ordered by phosphate, choline, and carbonyl groups. Water molecules form extensive hydrogen bonds with phosphate and carbonyl groups, but do not hydrogen bond with the choline group. Instead, they form a clathrate structure around the choline methyl group, (Pasenkiewicz-Gierula et al., 1997; Alper et al., 1993; Saiz and Klein, 2001). In a molecular dynamics study, Tobias (2001) showed that, mainly due to the orienting effect of negatively charged unesterized phosphate groups on water molecules, on average the dipoles of water molecules on the surface of fully hydrated lipid bilayers point toward the membrane surface. That is, water molecules on the surface of bilayers

are ordered and polarized. The ordering effect of these groups on water is embodied in the configuration of the hydrogen bond network. It is important to note that the hydrogen bond network is a dynamic structure. The motion of water molecules in the network can be resolved into two types: 1), local vibrations of individual water molecules about their equilibrium position in a given network configuration, which includes torsional rocking of the water molecule, chain stretching, and bond angle bending; 2), configurational movement of the network, i.e., relaxation of the network configuration with time (Stillinger and Weber, 1983). Both types of motion are constrained by the ordering of water molecules.

It can be shown (Bocian and Chan, 1978) that the order parameter of O-D bond S_D of D_2O determined by 2H NMR is a product of two order parameters:

$$S_D = S_\gamma S_N = (1/2) (3 \cos^2 \gamma - 1) \langle 1/2(3 \cos^2 \alpha - 1) \rangle \quad (2)$$

S_γ is the "order parameter" of the O-D bond relative to the orientation of the symmetry axis of the water molecule, i.e., the electric dipole of the water molecule, r_{dipole} , and S_N is the order parameter of the r_{dipole} relative to the normal to the bilayer, which is referred to as the network order parameter. The angular brackets imply ensemble averaging in Eq. 2. A nonzero value of S_N means that water molecules have a preferential orientation along the normal to the bilayer. In other words, the hydrogen bond network is oriented. However, the angle γ is about one-half of the bond angle of a water molecule, $109^\circ/2 = 54.5^\circ$, which is almost the magic angle, 54.7° ; i.e., the value of $1/2(3 \cos^2 \gamma - 1)$ is nearly zero (Gawrisch et al., 1992). This explains why the quadrupolar splittings $\Delta\nu$ of D_2O (proportional to S_D ; Seelig, 1977) are very small, even though the value of S_N could be large, as is expected to be in the case of dehydrated bilayers. (Molecular dynamics simulations showed that the effects of any flexibility of water molecules on the averaged structural properties of ion-water solution is negligible (Guardia and Padro, 1990). This suggests that vibrations of water molecule have no significant effect on the structure of the hydrogen bond network, such as in bilayers.) Because changes in the quadrupolar splitting of interbilayer D_2O are primarily due to changes in the value of S_N , the cusp pattern of the temperature variation of the quadrupolar splitting of interbilayer water around T_c reveals that the orientational ordering of interbilayer water molecules is lowest at T_c . This is consistent with how the orientational ordering of DPP-Tempo changes with temperature around the T_c of DOPC observed in the present study. Thus, instead of any contradiction between the 2H NMR and ESR measurements, we can accept a correlation between the ordering of the headgroup and the ordering of the interbilayer water. It is natural to expect that this correlation arises from the strong ionic and electrostatic interactions, such as the charge pair-

ing and hydrogen bonding between water molecules and headgroups explored by the molecular dynamic simulations.

The order parameter of the C-D bond in the $-CD_2-CD_2-$ group of the PC headgroup varies with temperature differently from the order parameter of water during the main phase transition, as mentioned in the Introduction. We believe that this is because the order parameter of the C-D bond in the $-CD_2-CD_2-$ group is primarily an intramolecular order parameter (Brown, 1996). That is, Hong et al. (1996) found that the conformation in which the $-CH_2-CH_2-$ moiety in the choline group and the beginning of *sn*-2 chain bend toward each other is significantly populated in the liquid crystalline phase of DMPC. This bend-back conformation of the $-CH_2-CH_2-$ moiety is likely due to its strong intramolecular interactions with the *sn*-2 carbonyl group, which renders the structure in the core of PC headgroup compact. As a result, the $-CH_2-CH_2-$ is not sensitive to the whole body motion of the headgroup. Moreover, there is no hydrogen bonding between water and the $-CH_2-CH_2-$ moiety (Wong and Mantsch 1988; Pasenkiewicz-Gierula et al., 1997). These might be possible reasons why the temperature variation of the quadrupolar splitting of the C-D bond in the $-CD_2-CD_2-$ group is different from that of the water molecules.

The effect of dehydration on the structure of lipid bilayers

The order parameters S_0 , S_2 and the rotational diffusion rates R_\perp , R_\parallel of DPP-Tempo in a DH DOPC dispersion are very close to those in a 10WT DOPC dispersion, except for the $12^\circ C$ down shift of T_c for the DH DOPC dispersion relative to the 10WT DOPC dispersion (cf. Figs. 5 and 7, also cf. Tables 1–4). However, the order parameters of DPP-Tempo in DH and 10WT DOPC dispersions are significantly larger than those in a FH DOPC dispersion before it is dehydrated, i.e., above T_f in the cooling cycle (cf. Table 1). Also, the R_\perp for the FH DOPC dispersion is substantially larger. (The R_\parallel , representing the internal rotation of the nitroxide moiety about the C-O bond, is hardly affected.) These results indicate that the dynamic structure in the headgroup region of DH and 10WT DOPC dispersions is similar, but is significantly different from that in the FH DOPC dispersion above T_f . Such features are most likely related to the fact that the water content in the bilayers, defined by the number of interbilayer water molecules per lipid (usually designated as n_w), is much lower in 10WT DOPC dispersion than in FH DOPC dispersions. These water molecules are capable of freely diffusing between the interbilayer and outside the vesicle regions.

10 wt % water in DOPC bilayers corresponds to each DOPC molecule being hydrated by 4.9 water molecules. In fully hydrated DOPC (DPPC) bilayers, each DOPC (DPPC) molecule can hold 32.5 (29.1) interbilayer water molecules (Tristram-Nagle et al., 1998; Nagle et al., 1996). But upon

freezing of bulk water, only 6–7 water molecules/lipid were found to be unfrozen in DPPC dispersions (Bach et al., 1982). These unfrozen water molecules are located in the interbilayer region (Gleeson et al., 1994). Because DOPC bilayers are slightly more hydrated than DPPC bilayers at room temperature, it is likely that the number of interbilayer water molecules per lipid in frozen DOPC dispersions could be slightly larger than 6–7, possibly 7–8. Such a number is reasonably close to 4.9 water molecules per lipid in 10WT DOPC dispersion, but it is much smaller than 32.5 water molecules per lipid in FH DOPC dispersion. Thus, about three-fourths of the water originally contained in the FH DOPC dispersion has been expelled from the interbilayer region into the frozen bulk water region below T_f . As we already mentioned, evidence for significant dehydration of DOPC bilayers upon freezing is also provided by the fact that the thickness of the polar region of frozen DOPC bilayers increases from 4 Å at -15°C to 10.5 Å at 0°C resulting from the melting of ice and rehydration of DOPC bilayers (Gleeson et al., 1994). The above comparisons suggest that large differences in the hydration between DH and 10WT DOPC dispersions on the one hand and the FH DOPC dispersion on the other hand are responsible for the large differences in the ordering and in R_\perp of DPP-Tempo in the corresponding dispersions.

The order parameters of DPP-Tempo in the dehydrated DOPC bilayers (DH DOPC and 10WT DOPC dispersions) are above 0.5, indicating that the headgroup region of dehydrated DOPC bilayers is highly ordered. This result is supported by a recent molecular dynamics study that shows that the phosphocholine group contributes a large positive potential to the increase in DOPC membrane dipole potential when the bilayers are substantially dehydrated (Mashl et al., 2001). Our observations are consistent with the effect of dehydration on the structure of lipid bilayers revealed from previous studies. Acyl chains in DLPC bilayers are crystallized and acyl chains in DSPC bilayers are solidified at temperatures above their normal phase transitions due to the osmosis-stress induced dehydration (Lis et al., 1982). POPC bilayers undergo a liquid crystalline to gel phase transition at 25°C as a result of dehydration (Binder and Gawrisch, 2001). The gel and fluid phases of POPE undergo a spontaneous dehydration and change to a crystalline phase (Seddon et al., 1984; Chang and Epand, 1983). The gel phase of n -saturated 1,2-diacylphosphatidylglycerols, when incubated at low temperatures, spontaneously transforms into quasicrystalline phases that are partially dehydrated (Zhang et al., 1997). Binding of calcium ions to PS bilayers dehydrates the phosphate group, and causes an isothermal crystallization of the acyl chains (Casal et al., 1987a,b; Dulhy et al., 1983). Similarly, binding of calcium ions to sphingomyelin dehydrates the headgroups, tightens the interlipid hydrogen bonding, and increases the gel to liquid crystalline transition temperature. All these observations consistently show that in dehydrated lipid bilayers, molec-

ular interactions between lipids are dramatically enhanced, leading to solidification of the lipid bilayers.

Water movement and osmotic effects

Dehydration or hydration of bilayers is a process of water moving between the interbilayer region and the bulk water phase. It is driven by a difference in chemical potential of water between the two regions. The water movement will stop when the chemical potentials of water in the two regions become equal again. Suppose just above the freezing point of the bulk water, the DOPC vesicles are in equilibrium with the bulk water. If the temperature is lowered to just below T_f the bulk water will freeze. No comparable phase transition has been observed for interbilayer water. The fact that water moves from the interbilayer region to the bulk would imply that the chemical potential of the frozen bulk water is reduced relative to that of interbilayer water below T_f . A reduction in the amount of interbilayer water leads to a substantial increase in the ordering of the interbilayer water, as evidenced by the large increase in S_0 observed for 4-PT in the interbilayer region below T_f . This would represent a decrease in entropy of the interbilayer water, and thereby an increase in its chemical potential relative to that of the frozen bulk water. This would have the effect of further driving water from the interbilayer region into the bulk water phase. A means whereby equilibrium can be restored between interbilayer and frozen bulk water would be if the pressure, P_i in the interbilayer region decreases to counterbalance the decrease in entropy. That is, a differential change in chemical potential $d\mu_{i,w}$ of the interbilayer water at constant temperature is given by $d\mu_{i,w} = v_{i,w} dP_i$, where $v_{i,w}$ is the partial molar volume of interbilayer water. Thus, a decrease in P_i will offset the initial decrease in entropy to bring the $\mu_{i,w}$ of the interbilayer water back into equality with μ_w , the chemical potential of the bulk water, thereby reestablishing equilibrium between them. (It is known that the value of $v_{i,w}$ depends on the degree of lipid hydration (White and King, 1985; Scherer, 1987). For lipid bilayers with n_w larger than 10 (i.e., the first hydration shell of the headgroup is filled), it is close to the commonly assumed value of the pure water, 30 \AA^3 , and does not change with the lipid hydration significantly (White and King, 1985). When n_w is below 10, $v_{i,w}$ decreases, becoming smaller than 30 \AA^3 , but remains positive (White and King, 1985). This only affects the magnitude, but not the sign of $v_{i,w} dP_i$).

In summary, in the model we propose, the water movement between the interbilayer and bulk water phase in DOPC vesicles is affected by the change in ordering of the interbilayer water (which is coupled with the change in ordering of the headgroups as the temperature varies), i.e., it is entropy driven. The water movement is opposed by the ensuing change in pressure in the interbilayer region. This is very similar to the well-known phenomenon of osmosis, i.e., water flows from an aqueous solution with a low concen-

tration of solute (high μ_w) into another aqueous solution with a high concentration of solute (low μ_w) yielding an osmotic pressure opposing the flow and eventually bringing μ_w in the two solutions into equality. We may define the osmotic pressure in the DOPC vesicles as the difference between the pressure in the interbilayer region (P_i) and atmospheric pressure (P_{atm}) outside the vesicle region, i.e., $P_i - P_{\text{atm}}$. Our model implies a negative osmotic pressure in the DOPC vesicles. In nature a negative pressure in an aqueous medium can be found in the sap in xylem conduct of plants (Steudle, 1995; Canny, 1998).

Gleeson et al. (1994) invoked the hydration force theory (Rand and Parsegian, 1989; Lis et al., 1982) to explain the water movement in DOPC vesicles. They suggested that changes in chemical potential of the interbilayer water with changes in the interbilayer separation are dominated by the work done by the hydration repulsion. In their treatment, the entropic term in the chemical potential of interbilayer water was not considered. The hydration force theory (Rand and Parsegian, 1989) is based upon Luzzati's (1968) model of the bilayer structure. That is, there is a clear-cut boundary between the headgroup layer and the water layer in the interbilayer region, and the structure of interbilayer water is the same as that of the bulk water. It implies that upon dehydration the structure of the interbilayer water in lipid bilayers remains unchanged. Luzzati's model is not consistent with our ESR observations that both interbilayer and bulk water molecules are locally ordered to different extents. In fact, we find that upon dehydration, changes in the ordering of interbilayer and bulk water are significantly different. Also, our ESR observations show that dehydration has a dramatic effect on the dynamic structure of the headgroup region of DOPC vesicles. Moreover, the structure of DOPC bilayers determined by combined x-ray and neutron diffraction measurements shows that there is a significant overlap of distributions of choline group from two opposing monolayers in the polar region (White and Wiener, 1995).

Implications of the conformational change of phosphoryl-Tempo on the reorganization of bilayers during the main phase transition

As shown above, when the temperature approaches T_c from either side (below or above), the phosphoryl-Tempo becomes increasingly disordered and the asymmetry of the ordering increases. These changes imply a continuous conformational change of DOPC headgroups (see Results). Conformational changes in the headgroup during the main phase transition of PC and PE bilayers were reported before. They include a shift of the orientation of the unique axis of the *sn*-2 chain ^{13}C O shielding tensor in the ripple phase of three PCs and DPPE bilayers (Wittebort et al., 1982; Wittebort et al., 1981), and a change in the orientation of ^{31}P O₄ in DPPC bilayers between 35° and 25°C (Campbell

et al., 1979). Because the ester carbonyl group, phosphate group, and the Tempo group in DPP-Tempo, are located at different depths of the headgroup region, it is likely that the whole headgroup changes its orientation, and it may be a general feature of the reorganization of the bilayer structure during the main phase transition. The cusp-like appearance around T_c of the ordering for DPP-Tempo that we observe implies that this change is related to critical fluctuations, as we discuss further below.

The structures of the DOPC headgroup and the phosphoryl-Tempo group in DPP-Tempo are different, and our ESR results cannot yield explicit details of how the conformation of a PC headgroup changes. Nevertheless, the conformational changes of both groups are likely associated with the same change in the structure of the hydrogen bond network, which may be inferred as follows. 1), A decrease in the ordering of the phosphoryl-Tempo group means an increase in the angular amplitude of the wobbling motion, which is indicative of a lateral expansion of the hydrogen bond network, i.e., an expansion of the surface area of DOPC bilayers. 2), As already shown above, as the temperature nears T_c , the rate of the flapping motion of the piperidine ring grows faster than that of the cutting motion. This suggests that changes in the structure of hydrogen bond network are likely to be anisotropic.

These changes in the structure of the headgroup region are consistent with optical and fluorescence microscopy observations that the size of vesicles increases during the main phase transition in both heating and cooling cycles (Yager et al., 1982; Bagotolli and Gratton, 1999). The ruffling of multilamellar vesicles during the phase transition observed from optical microscopy (Yager et al., 1982) might be caused by stresses in the bilayers, which are related to the increasing anisotropy in the dynamic structure in the headgroup region.

Anomalous swelling and critical density fluctuations

A continuous conformational change in the headgroups and disordering of both headgroups and interbilayer water at the main phase transition are very likely to be generally the case for PC bilayers. The sharp reduction in water ordering observed by NMR was interpreted in terms of a coupling between fluctuations in interbilayer water concentration and lateral density fluctuations in the headgroup region (Hawton and Doane, 1987). Our cusp-like results for the ordering of DPP-Tempo with respect to T_c indicate concomitant fluctuations in the structure of the headgroups. That is, at T_c , the ordering of headgroups and the ordering of interbilayer water are the lowest, and the swelling of the bilayers reaches a maximum. This is consistent with the conclusions of Honger et al. (1994), Chen et al. (1997), and Richter et al. (1999), that the anomalous swelling is caused by increased hydration of headgroups near the main phase transition, but inconsistent with the explanation that the

anomalous increase in the repeat distance of bilayers is due to the straightening of acyl chains (Zhang et al., 1995). Recall that we inferred from the x-ray diffraction data of DOPC vesicles (Gleeson et al., 1994) that acyl chains are also likely to be somewhat disordered around the main phase transition (see Results). In fact our ESR spectra from a chain spin label 5PC in DOPC vesicles do show significantly lower ordering around T_c than those at temperatures above or below T_c (data not shown). Thus it is possible that around the main phase transition of DPPC or DMPC bilayers, the increase in the thickness of the headgroup region, due to the swelling of polar headgroups, is larger than any thinning of the acyl chain region due to the disordering of acyl chains, such that the overall effect is a swelling of bilayers.

In considering the coupling between water concentration, lateral density fluctuations and structural changes of the headgroups in their quasicritical fluctuations near T_c , the osmosis model we suggested above might be of some relevance, because it correctly predicts the correlation between the reduced ordering of the headgroups and the interbilayer water with the water movement into the interbilayer region (i.e., anomalous swelling) as T_c is approached.

Changes in the repeat distance of DOPC bilayers during the main phase transition are complicated by the event of freezing of bulk water, which is close to the main phase transition. Because the number of interbilayer water molecules in the DH DOPC dispersions below T_f is much less than those in fully hydrated DPPC and DMPC bilayers, we expect that the amount of water, which can migrate between the interbilayer region and the bulk water region during the main phase transition, is substantially smaller than those in DPPC and DMPC bilayers. Thus, the effect of anomalous swelling is likely overshadowed by the effect of freezing-induced dehydration. This might explain why no swelling is observed for DOPC bilayers near the main phase transition.

Dehydration of membranes and membrane fusion

Our osmosis model implies that attractive forces induced by membrane dehydration facilitate the close contact between two membranes, which is a prerequisite for membrane fusion. Recently, Safran et al. (2001) suggested that the hydrophobic interaction between exposed acyl chains in the region of closely apposed membranes is responsible for the attractive forces between the fusing membranes, and that the exposure of the hydrophobic interior of the bilayers is caused by stresses in the bilayers. A recent molecular dynamics simulation study also showed that lipid acyl chains protrude from membranes in the closely apposed domain, which enhances the hydrophobic interaction between the membranes, thus initiating membrane fusion (Ohta-lino et al., 2001). However, the enhanced hydrophobic interactions between the fusing membranes cannot account for the role of osmotic swelling of secretory granules in exocytotic fusion, which has been the central

theme in the study of exocytosis for decades (Finkelstein et al., 1986; Holz, 1986).

Our osmosis model might be helpful in offering further insights into the swelling problem.

Origin of supercooling of bulk water

Why is the bulk water in DOPC vesicles supercooled? Gleeson et al. (1994) found that the T_f of water in DOPC vesicles does not depend on the experimental cooling rate. This suggests that the supercooling of bulk water is not due to a kinetic effect. Stillinger (1980) postulated that the clathrate-like structure in liquid water is responsible for supercooled water at atmospheric pressure. Aqueous solutions of tetraalkylammonium salts have been known for a long time to have some special properties that are important for the study of hydrophobic interactions in aqueous solutions (Lindenbaum, 1966, 1970; Blandamer, 1970; Kanno et al., 1989, 2001). One of the anomalies of these solutions is supercooling and glass formation, which is ascribed to the clathrate-like structure in these aqueous solutions (Kanno et al., 1989, 2001). Because the structure of the phosphatidylcholine group is similar to those of tetraalkylammonium salts, it is possible that a clathrate structure of water around the choline group in the PC headgroup (Pasenkiewicz-Gierula et al., 1997; Saiz and Klein, 2001) and the propagation property of the clathrate structure (Stillinger, 1980) are responsible for the supercooling of bulk water in FH DOPC dispersions. Such a local solvent structure may explain why the order parameter of 4-PT in the bulk water phase of DOPC vesicles is significantly greater than zero (cf. Fig. 10).

CONCLUSIONS

1. The ordering of the headgroups and the ordering of the interbilayer water in DOPC vesicles are correlated in the region of both the main phase transition, T_c and the freezing point, T_f . Both are inversely correlated with the degree of hydration of the bilayers, an observation most prominent in our work near T_f .
2. Given the observations near T_f , we have proposed a model in which increased ordering in the interbilayer region decreases its entropy and leads to (further) outflow of the interbilayer water until its pressure is reduced sufficiently to oppose further outflow, i.e., an osmosis model.
3. There is a continuous conformational change in the headgroups of DOPC bilayers around T_c , which is characterized by their decreasing ordering as the temperature approaches T_c from either direction. These changes represent a significant reorganization in the polar region of lipid bilayers around T_c . The cusp-like shape of the ordering about T_c is suggestive of quasicritical fluctuations in headgroup conformation near T_c , which

may be related to quasicritical behavior in other physical properties near T_c .

4. Addition of cholesterol to DOPC lowers T_f , but it continues to be the point at which the headgroup ordering increases. The addition of cholesterol has very little effect on the location of T_c or on the cusp-like shape of the ordering, which is rationalized in terms of limited interaction between cholesterol and unsaturated acyl chains of DOPC.

APPENDIX A: CARTESIAN ORDER PARAMETERS

The orientation of a biaxial spin label in a uniaxial solvent can be described by the Cartesian order parameters that are defined by a matrix (Luckhurst, 2000)

$$S_{\alpha\beta} = \langle (3I_{\alpha}I_{\beta} - \delta_{\alpha\beta})/2 \rangle, \quad (3)$$

where α and β are molecular axes of the spin label and I_{α} is the direction cosine between the α axis and the director. The matrix is symmetric, which follows from its definition and, in addition, the properties of the direction cosines mean that it is traceless,

$$\sum_{\alpha} S_{\alpha\alpha} = 0. \quad (4)$$

The relationship between the principal elements of the Cartesian order parameters and S_0 and S_2 are

$$S_{zz} = S_0, \quad (5)$$

and

$$S_{xx} - S_{yy} = \sqrt{\frac{3}{2}} S_2. \quad (6)$$

This work was supported by National Institutes of Health grants from the National Institute of General Medical Sciences and the National Center for Research Resources.

REFERENCES

- Alper, H. E., D. Bassolino-Klimas, and T. R. Stouch. 1993. The limiting behavior of water hydrating a phospholipid monolayer: a computer simulation study. *J. Chem. Phys.* 99:5547–5559.
- Arnold, K., A. Herrmann, K. Gawrisch, and L. Pratsch. 1987. Water-mediated effects of PEG on membrane properties and fusion. In *Molecular Mechanisms of Membrane Fusion*. S. Ohki, D. Doyle, T. D. Flanagan, S. W. Hui, and E. Mayhew, editors. Plenum Press, New York, NY and London, UK.
- Bach, D., B. Sela, and I. R. Miller. 1982. Compositional aspects of lipid hydration. *Chem. Phys. Lipids.* 31:381–394.
- Bagotolli, L. A., and E. Gratton. 1999. Two-photon fluorescence microscopy observation of shape changes at the phase transition in phospholipid giant unilamellar vesicles. *Biophys. J.* 77:2090–2101.
- Barnes, J. P., and J. H. Freed. 1998. Dynamics and ordering in mixed model membranes of dimyristoylphosphatidylcholine and dimyristoylphosphatidylserine: a 250-GHz electron spin resonance study using cholestane. *Biophys. J.* 75:2532–2546.
- Bechinger, B., and J. Seelig. 1991. Conformational changes of the phosphatidylcholine head groups due to membrane hydration. A ^2H -NMR study. *Chem. Phys. Lipids.* 58:1–5.
- Binder, H., and K. Gawrisch. 2001. Dehydration induces lateral expansion of polyunsaturated 18:0–22:6 phosphatidylcholine in a new lamellar phase. *Biophys. J.* 81:969–982.
- Binder, H., T. Gutberlet, A. Anikin, and G. Klose. 1998. Hydration of the dienic lipid dioctadecadienoylphosphatidylcholine in the lamellar phase—An infrared linear dichroism and x-ray study on headgroup orientation, water ordering, and bilayer dimensions. *Biophys. J.* 74:1908–1923.
- Blandamer, M. J. 1970. Structure and properties of aqueous salt solutions. *Quart. Rev.* 24:169–184.
- Bocian, D. F., and S. I. Chan. 1978. NMR studies of membrane structure and dynamics. *Annu. Rev. Phys. Chem.* 29:307–335.
- Brown, M. F. 1996. Membrane structure and dynamics studied with NMR spectroscopy. In *Biological Membranes. A Molecular Perspective from Computation and Experiment*. K. M. Merz, Jr. and B. Roux, editors. Birkhauser, Boston, MA.
- Brown, M. F., and J. Seelig. 1978. Influence of cholesterol on the polar region of phosphatidylcholine and phosphatidylethanolamine bilayers. *Biochemistry.* 17:381–384.
- Bryant, G., J. M. Pope, and J. Wolfe. 1992. Motional narrowing of the ^2H NMR spectra near the chain melting transition of phospholipid/D $_2\text{O}$ mixtures. *Eur. Biophys. J.* 21:363–367.
- Budil, D. E., S. Lee, S. Saxena, and J. H. Freed. 1996. Nonlinear-least-squares analysis of slow-motion EPR spectra in one and two dimensions using a modified Levenberg-Marquardt algorithm. *J. Magn. Res. A.* 120:155–189.
- Casal, H. L., H. H. Mantsch, and H. Hauser. 1987A. Infrared studies of fully hydrated saturated phosphatidylserine bilayers. Effect of Li^+ and Ca^{2+} . *Biochemistry.* 26:4408–4416.
- Casal, H. L., A. Martin, H. H. Mantsch, F. Paltauf, and H. Hauser. 1987B. Infrared studies of fully hydrated unsaturated phosphatidylserine bilayers. Effect of Li^+ and Ca^+ . *Biochemistry.* 26:7395–7401.
- Campbell, R. F., E. Meirovitch, and J. H. Freed. 1979. Slow-motional NMR line shapes for very anisotropic rotational diffusion. Phosphorus-31 NMR of phospholipids. *J. Phys. Chem.* 83:525–533.
- Canny, M. J. 1998. Transporting water in plants. *Am. Sci.* 86:152–159.
- Chang, H., and R. M. Epand. 1983. The existence of a highly ordered phase in fully hydrated dilauroylphosphatidylethanolamine. *Biochim. Biophys. Acta.* 728:319–324.
- Chen, F. Y., W. C. Hung, and H. W. Huang. 1997. Critical swelling of phospholipid bilayers. *Phys. Rev. Lett.* 79:4026–4029.
- Costa-Filho, A. J., Y. Shimoyama, and J. H. Freed. 2003. A 2D-ELDOR study of the liquid ordered phase in multilamellar vesicle membranes. *Biophys. J.* 84:2619–2633.
- Doniach, S. 1978. Thermodynamic fluctuations in phospholipid bilayers. *J. Chem. Phys.* 68:4912–4916.
- Dulhy, R. A., D. G. Cameron, H. H. Mantsch, and R. Mendelson. 1983. Fourier transform infrared spectroscopic studies of the effect of calcium ions on phosphatidylserine. *Biochemistry.* 22:6318–6325.
- Earle, K. A., J. K. Moscicki, A. Polimeno, and J. H. Freed. 1997. A 250 GHz ESR study of o-terphenyl: dynamic cage effects above T_c . *J. Chem. Phys.* 106:9996–10015.
- Finkelstein, A., J. Zimmer, and F. S. Cohn. 1986. Osmotic swelling of vesicles: its role in the fusion of vesicles with planar phospholipid bilayer membranes and its possible role in exocytosis. *Annu. Rev. Physiol.* 48:163–174.
- Gawrisch, K., D. Ruston, J. Zimmerberg, V. A. Parsegian, R. P. Rand, and N. Fuller. 1992. Membrane dipole potentials, hydration forces, and the ordering of water at membrane surfaces. *Biophys. J.* 61:1213–1223.
- Ge, M., and J. H. Freed. 1999. Electron-spin resonance study of aggregation of gramicidin in dipalmitoylphosphatidylcholine bilayers and hydrophobic mismatch. *Biophys. J.* 76:264–280.

- Ge, M., J. S. Cohen, H. A. Brown, and J. H. Freed. 2001. ADP ribosylation factor 6 binding to phosphatidylinositol 4,5-bisphosphate-containing vesicles creates defects in the bilayer structure: an electron spin resonance study. *Biophys. J.* 81:994–1005.
- Gleeson, J. T., S. Erramilli, and S. M. Gruner. 1994. Freezing and melting water in lamellar structures. *Biophys. J.* 67:706–712.
- Guardia, E., and J. A. Padro. 1990. Molecular dynamics simulation of single ions in aqueous solutions: effect of the flexibility of the water molecules. *J. Phys. Chem.* 94:6049–6055.
- Hauser, H., I. Pascher, R. H. Pearson, and S. Sundell. 1981. Preferred conformation and molecular packing of phosphatidylethanolamine and phosphatidylcholine. *Biochim. Biophys. Acta.* 650:21–51.
- Hawton, M. H., and J. W. Doane. 1987. Pretransitional phenomena in phospholipid/water multilayers. *Biophys. J.* 52:401–404.
- Ho, C., S. J. Slater, and C. D. Stubb. 1995. Hydration and order in lipid bilayers. *Biochemistry.* 34:6188–6195.
- Holz, R. W. 1986. The role of osmotic forces in exocytosis from adrenal chromaffin cells. *Annu. Rev. Physiol.* 48:175–189.
- Hong, M., K. Schmidt-Rohr, and H. Zimmermann. 1996. Conformation constraints on the headgroup and sn-2 chain of bilayer DMPC from NMR dipolar couplings. *Biochemistry.* 35:8335–8341.
- Honger, T., K. Mortensen, J. H. Ipsen, J. Lemmich, R. Bauer, and O. G. Mouritsen. 1994. Anomalous swelling of multilamellar lipid bilayers in the transition region by renormalization of curvature elasticity. *Phys. Rev Lett.* 72:3911–3914.
- Hwang, J. S., R. P. Mason, L.-P. Hwang, and J. H. Freed. 1975. Electron spin resonance studies of anisotropic rotational reorientation and slow tumbling in liquid and frozen media. III. Perdeuterated 2,2,6,6,-tetramethyl-4-piperidone N-oxide and an analysis of fluctuating torques. *J. Phys. Chem.* 79:489–511.
- Inoko, Y., and T. Mitsui. 1978. Structural parameters of dipalmitoyl phosphatidylcholine lamellar phases and bilayer phase transitions. *J. Phys. Soc. Jpn.* 44:1918–1924.
- Israelachvili, J. N., and H. Wennerstrom. 1992. Entropic forces between amphiphilic surfaces in liquids. *J. Phys. Chem.* 96:520–531.
- Kanno, H., H. Yokoyama, and Y. Yoshimura. 2001. A new interpretation of anomalous properties of water based on Stillinger's postulate. *J. Phys. Chem.* 105:2019–2026.
- Kanno, H., K. Shimada, and T. Katoh. 1989. A glass formation study of aqueous tetraalkylammonium halides solutions. *J. Phys. Chem.* 93:4981–4985.
- Lemmich, J., K. Mortensen, J. H. Ipsen, T. Honger, R. Bauer, and O. G. Mouritsen. 1995. Pseudocritical behavior and unbinding of phospholipid bilayers. *Phys. Rev. Lett.* 75:3958–3961.
- Lewis, R. N. A. H., and R. N. McElhaney. 1991. The mesomorphic phase behavior of lipid bilayers. In *The Structure of Biological Membranes*. P. Yeagle, editor. CRC Press, Boca Raton, FL.
- Lindenbaum, S. 1966. Thermodynamics of aqueous solutions of tetra-*n*-alkylammonium halides. Enthalpy and entropy of dilutions. *J. Phys. Chem.* 70:814–820.
- Lindenbaum, S. 1970. Thermodynamics of aqueous solutions of tetrabutylammonium carboxylates. Model systems for the hydrophobic interaction in protein. *J. Phys. Chem.* 75:3733–3737.
- Lis, L. J., M. N. Fuller, and R. P. Rand. 1982. Interactions between neutral phospholipid bilayer membranes. *Biophys. J.* 37:657–666.
- Luckhurst, G. R. 2000. Orientation order: distribution functions and order parameters (section 2.1). In *Physical Properties of Liquid Crystal: Nematics*. D. Dunmur, A. Fukuda, and G. R. Luckhurst, editors. IEE Publishing, London, UK.
- Luzzati, V. 1968. X-ray diffraction studies of lipid-water systems. In *Biological Membranes. Physical Facts and Function*. D. Chapman, editor. Academic Press, New York, NY.
- Mashl, R. J., H. L. Scott, S. Subramaniam, and E. Jacobsson. 2001. Molecular simulation of dioleoylphosphatidylcholine lipid bilayers at differing levels of hydration. *Biophys. J.* 81:3005–3015.
- Meirovitch, E., D. Igner, G. Moro, and J. H. Freed. 1982. Electron-spin relaxation and ordering in smectic and supercooled nematic liquid crystals. *J. Chem. Phys.* 77:3915–3938.
- Meirovitch, E., A. Nayeem, and J. H. Freed. 1984. Analysis of protein-lipid interactions based on model simulations of electron spin resonance spectra. *J. Phys. Chem.* 88:3454–3465.
- Mitaku, S., T. Jippo, and R. Kataoka. 1983. Thermodynamic properties of the lipid bilayer transition. Pseudocritical phenomena. *Biophys. J.* 42:137–144.
- Nagle, J. F. 1980. Theory of the main lipid bilayer phase transition. *Annu. Rev. Phys. Chem.* 31:157–195.
- Nagle, J. F., R. Zhang, S. Tristram-Nagle, W. Sun, H. I. Petrache, and R. M. Suter. 1996. X-ray structure determination of fully hydrated L_{α} phase dipalmitoylphosphatidylcholine bilayers. *Biophys. J.* 70:1419–1431.
- Nagle, J. F., and H. L. Scott, Jr. 1978. Lateral compressibility of lipid mono- and bilayers. Theory of membrane permeability. *Biochim. Biophys. Acta.* 513:236–243.
- Ohta-lino, S., M. Pasenkiewicz-Gierula, Y. Takaoka, H. Miyagawa, K. Kitamura, and A. Kusumi. 2001. Fast lipid disorientation at the onset of membrane fusion revealed by molecular dynamics simulations. *Biophys. J.* 81:217–224.
- Papahadjopoulos, D., K. Jacobson, S. Nir, and T. Isac. 1973. Phase transition in phospholipid vesicles. Fluorescence polarization and permeability measurements concerning the effect of temperature and cholesterol. *Biochim. Biophys. Acta.* 311:330–348.
- Pasenkiewicz-Gierula, M., Y. Takaoka, H. Miyagawa, K. Kitamura, and A. Kusumi. 1997. Hydrogen bonding of water to phosphatidylcholine in the membrane as studied by a molecular dynamics simulation: location, geometry, and lipid-lipid bridging via hydrogen-bonded water. *J. Phys. Chem. A.* 101:3677–3691.
- Pasenkiewicz-Gierula, M., Y. Takaoka, H. Miyagawa, K. Kitamura, and A. Kusumi. 1999. Charge pairing of headgroups in phosphatidylcholine membranes: a molecular dynamics simulation study. *Biophys. J.* 76:1228–1240.
- Pope, J. M., L. Walker, B. A. Cornell, and G. W. Francis. 1981. NMR study of synthetic bilayers in the vicinity of the gel-liquid-crystal transition. *Biophys. J.* 35:509–520.
- Rand, R. P., D. Chapman, and K. Larsson. 1975. Tilted hydrocarbon chains of dipalmitoyl lecithin become perpendicular to the bilayer before melting. *Biophys. J.* 15:1117–1124.
- Rand, R. P., and V. A. Parsegian. 1989. Hydration forces between phospholipids bilayers. *Biochim. Biophys. Acta.* 988:351–376.
- Richter, F., L. Finegold, and G. Rapp. 1999. Sterols sense swelling in lipid bilayers. *Phys. Rev. E.* 59:3483–3491.
- Safran, S. A., T. L. Kuhl, and J. N. Israelachvili. 2001. Polymer-induced membrane contraction, phase separation, and fusion via Marangoni Flow. *Biophys. J.* 81:659–666.
- Saiz, L., and M. L. Klein. 2001. Structural properties of a highly polyunsaturated lipid bilayer from molecular dynamics simulations. *Biophys. J.* 81:204–216.
- Scherer, J. R. 1987. The partial molar volume of water in biological membranes. *Proc. Natl. Acad. Sci. USA.* 84:7938–7942.
- Schneider, D. J., and J. H. Freed. 1989. Calculating slow motional magnetic resonance spectra: a user's guide. In *Spin Labeling Theory and Applications*, Vol. 8. L. J. Berliner and J. Reuben, editors. Plenum Press, New York, NY. 1–76.
- Seddon, J. M., G. Cevc, R. D. Kaye, and D. Marsh. 1984. X-ray diffraction study of the polymorphism of hydrated diacyl- and diacylphosphatidylethanolamines. *Biochemistry.* 23:2634–2644.
- Seelig, J. 1977. Deuterium magnetic resonance: theory and application to lipid membranes. *Q. Rev. Biophys.* 10:353–418.
- Stedle, E. 1995. Trees under tension. *Science.* 378:663–664.
- Stillinger, F. H. 1980. Water revisited. *Science.* 209:451–457.
- Stillinger, F. H., and T. A. Weber. 1983. Inherent structure in water. *J. Phys. Chem.* 87:2833–2840.

- Tobias, D. 2001. Membrane simulations. *In Computational Biochemistry and Biophysics*. O. M. Becker, A. D. MacKerell, B. Roux, and M. Watanabe, editors. Marcel Dekker, Inc., New York, NY.
- Tristram-Nagle, S., H. I. Petrache, and J. F. Nagle. 1998. Structure and interactions of fully hydrated dioleoylphosphatidylcholine bilayers. *Biophys. J.* 75:917–925.
- Tsuchida, K., and I. Hatta. 1988. ESR studies on the ripple phase in multilamellar phospholipids bilayers. *Biochim. Biophys. Acta.* 945: 73–80.
- Ulrich, A. S., M. Sami, and A. Watts. 1994. Hydration of DOPC bilayers by differential scanning calorimetry. *Biochim. Biophys. Acta.* 1191: 225–230.
- Westerman, P. W., M. J. Vaz, L. M. Strenk, and W. Doane. 1982. Phase transitions in phosphatidylcholine multibilayers. *Proc. Natl. Acad. Sci. USA.* 79:2890–2894.
- White, S. H., and G. I. King. 1985. Molecular packing and area compressibility of lipid bilayers. *Proc. Natl. Acad. Sci. USA.* 82:6532–6536.
- White, S. H., and M. C. Wiener. 1995. Determination of the structure of fluid lipid bilayer membranes. *In Permeability and Stability of Lipid Bilayers*. E. A. Disalvo and S. A. Simon, editors. CRC Press, Boca Raton, FL.
- Wittebort, R. J., A. Blume, T.-H. Huang, S. K. Das Gupta, and R. G. Griffin. 1982. Carbon-13 nuclear magnetic resonance investigation of phase transition and phase equilibria in pure and mixed phospholipid bilayers. *Biochemistry.* 21:3487–3502.
- Wittebort, R. J., C. F. Schmidt, and R. G. Griffin. 1981. Solid-state carbon-13 nuclear magnetic resonance of the lecithin gel to liquid-crystalline phase transition. *Biochemistry.* 20:4223–4228.
- Wong, P. T. T., and H. H. Mantsch. 1988. High-pressure infrared spectroscopic evidence of water binding sites in 1,2-diacyl phospholipids. *Chem. Phys. Lipids.* 46:213–224.
- Wu, S. H., and H. M. McConnell. 1973. Lateral phase separations and perpendicular transport in membranes. *Biochem. Biophys. Res. Commun.* 55:484–491.
- Yager, P., J. P. Sheridan, and W. L. Peticolas. 1982. Changes in size and shape of liposomes undergoing chain melting transitions as studied by optical microscopy. *Biochim. Biophys. Acta.* 693:485–491.
- Zhang, Y. P., R. N. A. H. Lewis, and R. N. McElhaney. 1997. Calorimetric and spectroscopic studies of the thermotropic phase behavior of *n*-saturated 1,2-diacylphosphatidylglycerols. *Biophys. J.* 72:779–793.
- Zhang, R., W. Sun, S. Tristram-Nagle, R. L. Herdrick, R. M. Suter, and J. F. Nagle. 1995. Critical fluctuations in membranes. *Phys. Rev. Lett.* 74:2832–2835.